# CLEAN AND EFFICIENT ENERGY CONVERSION PROCESSES (CECON-PROJECT)


| | |
|---|---|
| Gaz de France | Mrs M. J. Fourniguet, Mrs I. Alliat |
| BG plc | Mr K. Shepherd, Mr S. Matthews |
| Danish Gas Technology Centre | Mr A.N. Myken, Mr P. Andersen |
| Katholieke Universiteit Leuven | Mr E. van den Bulck |
| N.V. ACOTECH S.A. | Mr P. Vansteenkiste |
| N.V. Nederlandse Gasunie | Mr G. Tiekstra |

N.V. Nederlandse Gasunie Mr O. Florisson (project coordinator)



CONTRACT JOE 3-CT95-0011


# Final Report (Public)

1st February 1996 - 31st March 1998


Research funded in part by
**THE EUROPEAN COMMISSION**
in the framework of the Non Nuclear Energy Programme
JOULE III

Table of contents

## 1. EXECUTIVE SUMMARY

*Industrial objectives and strategic aspects*

Around one quarter of the total industrial energy use within the fifteen European Union countries is associated with furnaces, kilns and ovens operating at 400EC and upward. Equipment for heat recovery in the form of metallic recuperators, recuperative burners and regenerative burners has been available commercially for many years and these can save up to 65% of the energy used in these processes. However, this equipment has only been exploited within small sectors of the process industries, representing about 4% of the total.

The reasons for this low penetration of heat recovery systems are high capital cost, high installation cost, especially for retro-fitting on existing processes, large size of heat recovery equipment relative to the space available on many processes and the high cost of control and ancillary equipment for regenerative systems.

The objectives of the work programme reported are the development and testing of two optimised energy conversion processes, both consisting of a radiant surface gas burner and a ceramic heat exchanger.

The first sub-objective of the programme is related to industrial heating, drying and curing processes requiring low and medium heat fluxes. It is estimated that around one tenth of the total EC industrial energy use is associated with such processes. The majority of these processes currently use convection and conduction as the main heat transfer mechanisms and overall energy efficiencies are typically below 25%. For many drying and finishing processes (such as curing powder coatings and drying paints, varnishes, inks, and for the fabrication of paper and textiles), radiant heating can achieve much faster drying rates and higher energy efficiency than convective heating.
In the project new concepts of natural gas fired radiant heating have been investigated which would be much more efficient than the existing processes. One element of the programme was the development of gas burners having enhanced radiant efficiencies. A second concerned the investigation of the safety of gas burners containing significant volumes of mixed gas and air. Finally the new gas burners were tested in combination with the high temperature heat exchanger to create highly efficient radiant heating systems.

The second sub-objective concerned the development of a compact low cost heat exchanger capable of achieving high levels of heat recovery (up to 60%) which could be easily installed on industrial processes. This would make heat recovery a practical proposition on processes where existing heat recovery technology is currently not cost effective.

The project will have an impact on industrial processes consuming around 80 MTOE of energy per year within EU countries (1 MTOE equals 41.8 PJ). The overall energy saving potential of the project is estimated to be around 22 MTOE which is around 10% of the total energy consumed by industry in the EU. This energy saving corresponds to a reduction in carbon dioxide emissions of around 45 million tons.

The project has developed technologies which will lead to products which reduce energy consumption and hence $CO_2$-emissions. The radiant burners have very low $NO_X$-emissions and will make an important contribution to air quality. The results from this project will contribute to the development of expertise within the Community and to the retention of employment through their production and exploitation.

*Technical achievements*

The objective of the project was the development of a gas powered radiant surface burner with internal recuperation, that has a high efficiency and low emission. This clean and efficient energy conversion process is a combination of two units: a **radiant surface gas burner** (first sub-objective) and a **ceramic heat exchanger** (second sub-objective) to preheat the combustion air by the flue gas.

Two types of radiant surface gas burners have been developed within this project: a premix radiant surface burner a non-premix radiant surface burner:

* The **premix radiant surface gas burner** is constructed of a ceramic housing and of a metallic fibre mat used as the burner surface. This burner has been tested successfully with two different surface structures (knitted and sintered). Endurance tests of the burners, in which the most severe operational conditions were simulated (surface temperature 1000 $^{o}$C), showed that no ageing or degradation of the burner surfaces occurred after tests of 6 months (corresponding to 2 years operation under the design conditions).
  A safety device has been developed to reduce the risks of premature ignition of the gas-air mixture within the premix burner. For an enclosed radiant burner the size of the pressure-upset depends upon the ratio of the volume of the air/gas mixture that is ignited to the total burner-system volume (burner + cover + heat exchanger). A design rule to predict the resulting pressure peak height has been postulated. The safety device consisting of a ceramic foam which fills up the volume in the burner but, due to its porous structure, lets the gas-air mixture pass through with only a small pressure drop. The design rule has been validated by comparison of the results of explosion tests with the safety device and the results without the safety device. Also the influence of preheat of the gas/air mixture (up to 500 °C) on the pressure peak height has been determined. Explosion tests showed that this device acts satisfactory and that the design rule is valid up to temperatures of the gas/air mixture up to 500 °C.

* The **non-premix radiant surface burner powered with natural gas** has been designed for high temperature conditions (furnace temperatures above 800 $^{o}$C and preheat temperature of the combustion air up to 1000 $^{o}$C). A study into materials suitable for the non-premix radiant burner has been carried out and further to this different designs of the burner have been tested by numerical simulation of flow, combustion and radiation of the burner with the CFD-code TUFCA. The most promising design has been used for the prototypes constructed.
  Tests of the prototypes showed a serious problem inherent to the design: the fuel gas cracked prior to the injection into the combustion chamber because it was excessively heated to much by the preheated air. The soot formed by the cracking seriously polluted the inner burner.

Alternative designs in which the fuel gas was not heated have been established. The concept operated satisfactorily without preheating of the combustion air, although $NO_X$-emissions were high. However, when the combustion air was preheated to 400°C, the burner broke down.

The second sub-objective concerned the development of a **ceramic heat exchanger**. For the prediction of the thermal and flow characteristics of the heat exchanger, a computer model has been developed, and validated by dedicated tests.
Pressure drop experiments have been performed on thick finned heat exchanger surfaces, such as those that occur in flue gas heat exchangers. It appeared that the fact that the fins were not continuous strips of solid material did not affect the friction-factor/Reynolds-number correlation. Furthermore it was shown that about 20 to 25 % of the installed heat exchanger surface can be 'lost' due to flow channelling when the fin tips are separated. The offset fin arrangement yields a 10 to 15 % higher friction factor for the range of Reynolds number of 2000 to 4000. This range is representative of the flue gas flow.
Ceramic heat exchangers for heat inputs of 100 kW and 50 kW have been designed. Experimental validation of their performance showed that the pressure drops are much lower than can be explained by the established theory. The thermal exchange performance suffered from excess heat losses which made it not possible to estimate the heat transfer correlations accurately.

A modular ceramic high temperature heat exchanger has been developed and tested, including extensive material testing. The material testing showed that at up to 1300 $^oC$ the ceramic material used for the heat exchanger elements (CarSIK-NT (trade name) reaction bonded silicon carbide, RBSC) has excellent properties (strength retention, good oxidation resistance to oxidising environments, resistance to thermal shock and thermal cycling). High temperature ceramic adhesives showed strong joints between RBSC specimens as well as a good resistance to high temperature oxidation.
A counterflow heat exchanger using RBSC elements has been designed, fabricated and assembled. The heat exchanger has been tested and has been successfully operated up to a flue gas temperature of ~1400 $^oC$. The pressure drops measured for this design of heat exchanger are low, and an effectiveness of ~ 70% has been determined for this design of heat exchanger.

The combustion air preheating process (« CECON Unit ») has been validated with the two premix gas burners utilising internal recuperation. The capacity of the prototype process developed is around 50 kW (in terms of (natural) gas input).

To collect the combustion products from the radiant surface burners a dedicated enclosure casing was designed. In front of the burner a window of quartz glass was mounted. The heat exchanger was coupled to the outlet of the enclosed burner. The air preheated by using the heat exchanger was transferred to the external mixer via stainless steel pipes.
The major difficulty encountered in the construction of the « CECON Unit » was caused by the large dimensions and heavy weight of the ceramic heat exchanger.

Two different versions of the « CECON Unit » have been assembled and tested, corresponding to the premix radiant surface gas burners with the two different types of burner mats developed.

The two premix radiant surface gas burners have been characterised both, in the open air and as a part

of the two « CECON Units », in terms of radiant efficiency (the ratio of the radiant flux emitted to the power consumed). In addition, tests were performed on the enclosed perforated burner with cold air (i.e. without the heat exchanger). All the tests were performed using the burners in a downward vertical emission position.

The radiant efficiency of both types of burners operating in the open (so not-enclosed) were similar, i.e. 44% for a power density of 250 kW(NCV)/m². Both « CECON Units » also produced similar results to each other, with an efficiency of about 60% for a power density of 250 kW(NCV)/m² and a combustion air preheat temperature of 200 $^{o}$C. This was 15 points above the efficiency of non-enclosed burners (so, a relative increase of ca 35%).

Tests on the enclosed perforated gas burner with cold air (i.e. without the heat exchanger) showed that at the same power density the radiant efficiency was approximately 6 points lower than the efficiency measured with the combustion air at 200°C, i.e. 54% instead of 60%.
These results proved the clear value in the recuperation of the energy in the combustion products to preheat the combustion air in order to increase the radiant efficiency. With higher preheated air temperatures (which was not possible to obtain due to a large air leakage in the heat exchanger) it could have been possible to increase the efficiency even more.

Further to this, the $NO_X$-emission of the premix radiant gas burners coupled with the heat exchanger (« CECON Unit ») were rather low, at less than 10 ppm at 3% $O_2$. The emission of CO was negligible.

So the « CECON Unit » developed in the CECON-project really represents a Clean and Efficient Energy Conversion Process.

Although this project proved the principle of the « CECON Unit » the size and weight of the heat exchanger are not compatible with a direct industrial application of a enclosed radiant surface burner. Some additional work is needed to design a more compact system which is easier to manufacture.

## 2. PARTNERSHIP

The parties to the project and their contact persons have been given the following table.

| **Party** | **Contact person** |
|---|---|
| *(Project coordinator)*<br>N.V. Nederlandse Gasunie<br>P.O. box 19<br>Concourslaan 17<br>9700 MA Groningen<br>The Netherlands | Mr O. Florisson<br>telephone: +31 50 521 26 51<br>fax: +31 50 521 1978<br>email: o.florisson@gasunie.nl |
| N.V. Acotech S.A.<br>Bekaertstraat 2<br>B-8550 Zwevegem<br>Belgium | Mr P. Vansteenkiste<br>telephone: +32 56 76 64 61<br>fax: +32 56 76 64 63<br>email: vansteenkiste_philip@acotech.be |
| Katholieke Universiteit Leuven<br>Department Werktuigbouwkunde<br>Celestijnenlaan 300A<br>B-3001 Heverlee<br>Belgium | Prof. Dr. Ir. E. van den Bulck<br>telephone: +32 16 32 25 09<br>fax: +32 16 32 25 98<br>email: erik.vandenbulck@mech.kuleuven.ac.be |
| BG plc<br>Gas Research & Technology Centre<br>Ashby Road,<br>Loughborough<br>Leicestershire<br>LE11 3GR<br>United Kingdom | Mr K. Shepherd<br>telephone: +44 15 09 28 27 65<br>fax: +44 15 09 28 31 44<br>email: karl.shepherd@bgtech.co.uk |
| Danish Gas Technology Centre a/s<br>Dr. Neergaards Vej 5A<br>DK-2970 H✓rsholm<br>Denmark | Mr A. N. Myken<br>telephone: +45 45 76 60 44<br>fax: +45 45 76 70 15<br>email: amy@dgc.dk |
| Gaz de France<br>Direction de la Recherche-Centre d'Essais et de Recherches sur les Utilisations du Gaz<br>361, av du Pr sident Wilson<br>BP 33<br>93 211 Saint Denis La Plaine CEDEX<br>France | Mrs M.J. Fourniguet<br>telephone: +33 1 49 22 59 75<br>fax: +33 1 49 22 55 63<br>email: marie-jose.fourniguet@edfgdf.fr |

**Table 2.1: Participating companies and contact persons**

## 3. OBJECTIVES OF THE PROJECT

Around one quarter of the total industrial energy use within the fifteen European Union countries is associated with furnaces, kilns and ovens operating at 400EC and upward. Equipment for heat recovery in the form of metallic recuperators, recuperative burners and regenerative burners has been available commercially for many years and these can save up to 65% of the energy used in these processes. However, this equipment has only been exploited within small sectors of the process industries, representing about 4% of the total.

The objectives of the work programme reported are the development and testing of two optimised energy conversion processes, both consisting of a **radiant surface gas burner** and a **ceramic heat exchanger.**

The first sub-objective of the programme is related to natural gas fired **burners** for industrial heating, drying and curing processes requiring low and medium heat fluxes. It is estimated that around one tenth of the total EC industrial energy use is associated with such processes. The majority of these processes currently use convection and conduction as the main heat transfer mechanisms and overall energy efficiencies are typically below 25%. For many drying and finishing processes (such as drying paints, varnishes, inks and curing powder coatings), radiant heating can achieve much faster drying rates and higher energy efficiency than convective heating.

One element of the programme was the development of natural gas fired burners having enhanced radiant efficiencies. A second concerned the investigation of the safety of gas burners containing significant volumes of mixed gas and air. Finally the new burners were tested in combination with the high temperature heat exchanger to create highly efficient radiant heating systems.
Two types of radiant surface burners are developed within this project: a premix radiant surface burner and a non-premix radiant surface burner. The premix surface burner was tested with two different surface structures.

The second sub-objective was the development of a compact low cost **heat exchanger** capable of achieving high levels of heat recovery (up to 60%) which could be easily installed on industrial processes. This would make heat recovery a practical proposition on processes where existing heat recovery technology is currently not cost effective.

The high temperature heat exchanger was developed to preheat the combustion air for the radiant burners by the combustion gases.
The key to the development of such a heat exchanger is the selection and proving of adequately reliable high temperature ceramics. While all possibilities have been considered, the design has been based on reaction bonded silicon carbide.

The combustion air preheating process is validated with the two premix gas burners utilising internal recuperation. The capacity of the prototype process is around 50 kW (in terms of (natural) gas input).

So, the design objectives for the integrated energy conversion processes are:

- High thermal efficiency (> 85%)
- Low pollutant emissions ($NO_X$ < 25 ppm)
- Compact design (< 8 dm3/kW)
- Low price (400-500 ECU/kW)
- Competitive with electrical designs
- Intrinsic safe

From this, the following aims have been formulated:

1 Development of a safety device that reduces the explosion risks for premix radiant surface burners.

2 Development of two premix radiant surface burners equipped with two kinds of economical metal fibre mats.

3 Development of a non-premix radiant surface burner, suitable for high temperature conditions, i.e. high furnace temperatures (above 800 $^oC$) and high preheat temperatures (up to 700 $^oC$).

4 Development of a model for a ceramic heat exchanger, for heating air up to 700 $^oC$ by flue gas (temperatures up to 1400 $^oC$)

5 Development of a ceramic heat exchanger, capable of operating on processes up to 1400 $^oC$.

6 Validation of both prototype premix burners with internal recuperation, i.e. of both combinations of premix radiant surface burners and ceramic heat exchanger.

The project will have an impact on industrial processes consuming around 80 MTOE of energy per year within EU countries (1 MTOE equals 41.8 PJ). The overall energy saving potential of the project is estimated to be around 22 MTOE which is around 10% of the total energy consumed by industry in the EU. This energy saving corresponds to a reduction in carbon dioxide emissions of around 45 million tons.

The project has developed technologies which will lead to products which reduce energy consumption and hence $CO_2$-emissions. The radiant burners have very low $NO_X$-emissions and will make an important contribution to air quality. The products which flow from this project will contribute to the development of expertise within the Community and to the retention of employment through their production and exploitation.

## 4. SCIENTIFIC AND TECHNICAL DESCRIPTION OF THE PROJECT

### 4.1 Construction of the Project

The project has been constructed from 6 Tasks (excluding project coordination), cohering as indicated in figure 4.1.1

**Figure 4.1.1: Coherence of the Tasks of the project**

The Tasks and the corresponding parties responsible for the Tasks are:

| **Task no** | **Task title** | **Responsible party** | **Assisting party** | **Status** |
|---|---|---|---|---|
| - | Project Coordination | N.V. Nederlandse Gasunie | | Contractor |
| 1 | Safety Design for Premix Surface Burners | N.V. Nederlandse Gasunie | | Contractor |
| 2 | Development of the Premix Surface Burner | N.V. Acotech S.A | | Associated-Contractor |
| 3 | Development of the Non-Premix Surface Burner | Danish Gas Technology Centre a/s | | Contractor |
| 4 | Modelling of the Ceramic Heat Exchanger | Katholieke Universiteit Leuven, | | Contractor |
| 5 | Development of the Ceramic Heat Exchanger | BG plc | Gaz de France | Contractor |
| 6 | Validation of the Burners with Internal Recuperation | Gaz de France | | Contractor |

**Table 4.1.1: The Tasks and the parties to the project**

Please note that the “assisting party” indicated in the table gave a significant contribution to the execution of the Task led by the “responsible party”.

## 4.2 Task 1, Safety Design for Premix Surface Burners

(Contractor: N.V. Nederlandse Gasunie)

### 4.2.1 Introduction

Within a premix radiant burner there exists a flammable mixture of gas and air just below the burner deck. In a case where the burner deck is ruptured there is a possibility that this mixture below the burner deck will ignite. Results of previous experiments performed with a radiant burner in a boiler showed that relatively high pressure upsets could result. These pressures could cause damage to e.g. the boiler structure. The size of the pressure-upsets depends upon the ratio of the volume of the gas that is ignited to the total boiler volume. In general, a pressure limit of 100 mbar is regarded as safety limit. At pressures above this level windows start breaking and personal injuries due to flying fragments could occur.

Within the CECON-project the objective of Task 1 is to develop a safety-device to reduce the explosion risk for premix radiant burners. The basic principle followed for this device is to reduce the risk by reducing the amount of gas-air mixture that can be ignited prematurely.

For a closed radiant burner the size of the pressure-upset depends upon the ratio of the volume of the air/gas mixture that is ignited to the total burner-system volume (burner + cover + heat exchanger). A design rule to predict the resulting pressure peak height has been postulated.

In this Task a safety-device has been developed and tested. The design rule has been validated by comparison of the results of explosion tests with the safety device and the results without the safety device. Also the influence of preheat of the gas/air mixture (up to 500 °C) on the pressure peak height has been determined.

### 4.2.2 Description of the Objects and Subjects for the Test

#### 4.2.2.1 The Burner

The burner tested for the Task 1 of the CECON-project is a closed premix radiant burner with a metal fibre burner deck (Acotech AC 200 P1)(see figure 4.2.1).

For testing purposes the burner was closed by a metal plate with heat resisting capacities. (Avesta).
In practice the burner will be closed by an expensive ceramic material with good radiant characteristics.
The volume indicated by $V_G$ is 13 l.(7*26*72.5 cm) The volume indicated by $V_T$ is 22 l.(11.5*26.5*72.5 cm)
The capacity of the burner is 50 kW. Air is supplied by a fan and gas containers are is used to supply the natural gas at the test site.

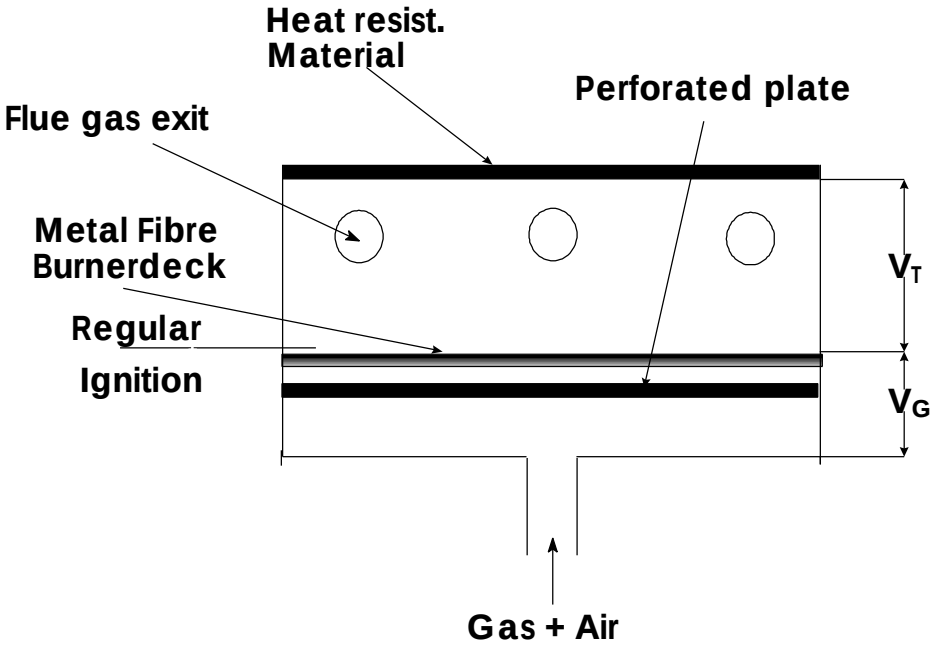


**Figure 4.2.1: Schematic drawing of closed burner system without safety measure.**

The safety consideration is that due to a rupture of the burner deck flashback may occur and the gas/air mixture volume $V_G$ will be ignited. Due to the expanding flue gases a pressure build up will be realised. This could damage the structure (plate), or even cause a safety risk for people in the vicinity of the burner system.
In the burner developed in the CECON-project combustion air is preheated by the exhaust gases in a specially developed ceramic heat exchanger. This heat exchanger causes a flow resistance. This effect is simulated in the explosion test by closing 4 of the 6 exhaust openings and reducing the diameter of the remaining openings.

#### 4.2.2.2 Design Rule

With respect to resulting max. pressures after an explosion a design rule was derived :

$$P_{\max}(mbar) = 6400 * f * \frac{V_G}{V_T}$$

with:
6400 = expansion factor to compensate for the ratio of combustion gases to fuel gas etc. for natural gas;
$f$ = factor to compensate for leakage. For a fully closed volume $f$ has a value of 1;
$V_G$= volume of gas that is ignited;
$V_T$= (total) volume into which the resulting flue gases will expand.
The expansion factor (6400) is a function of the composition of the gas, gas/air ratio and the conditions (P, T) of the gas. It is possible to calculate the expansion factor a priori, see ref. [2].

In most calculations the leakage factor $f$ is taken to be 1 as a worst case scenario. In the case of the empty test burner $f$ equals $6*10^{-3}$. So putting $f$ equal to 1 leads to a over estimation of the occurring max. pressures by a factor 170.
On the other hand $f$ is very hard to predict a priori. $f$ tends to change also as function of the pressure level due to the damage done to the construction (extra leaks) and $f$ is also affected by the intensity of the ignition.

#### 4.2.2.3 Safety Measure

From the design rule it follows that a lower ratio $V_G/V_T$ leads to lower max. pressure levels. The safety device lowers the ratio by reducing $V_G$ and increasing $V_T$.
This is accomplished by the introduction of a layer of ceramic foam of 4.0 cm thickness just below the perforated plate. Please see figure 4.2.2.

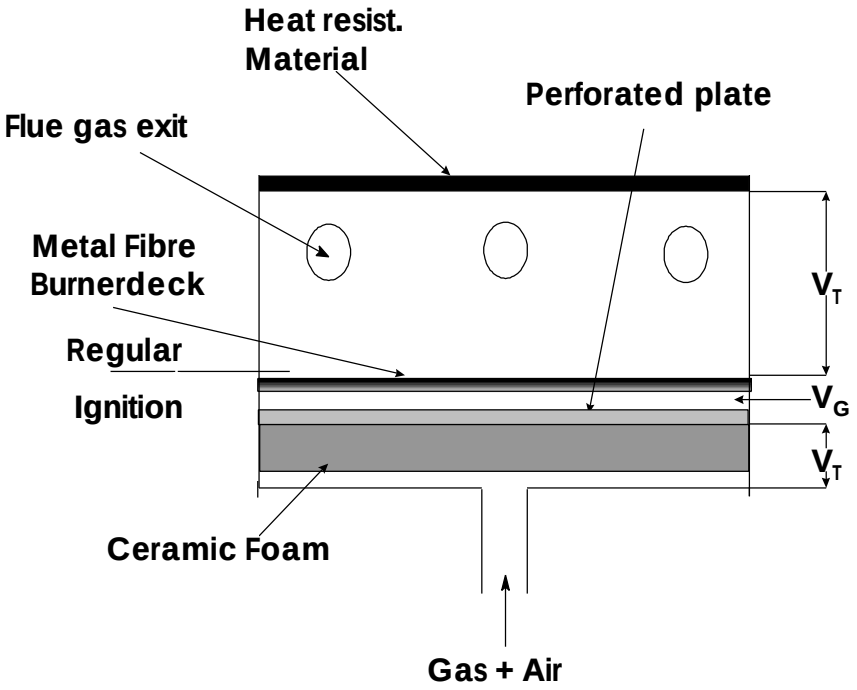


**Figure 4.2.2: Schematic drawing of a closed burner system with safety measure.**

The ceramic foam has a porosity of 90%. Due to the high porosity the pressure loss will be low so the capacity of the burner is not affected significantly. This particular foam structure is characterised by a random orientation of the pores. In this way a better flow distribution is reached. The diameter of the pores is typically around 0.6 mm. It is used as a material for burner decks and has good flame arresting capabilities.
As $V_G$ is reduced to 1.9 l and $V_T$ is increased up to 33 l the volume ratio with the safety measure is 0.1 times the volume ratio for the "empty" burner.
The manufacturer of the ceramics (ECO-Ceramics) supplies the foam in layers of min. 1.3 mm thickness. For the test 3 layers are used (3.9 mm thickness).

#### 4.2.2.4 Preheat Temperature

Preheat of the gas/air mixture has two main effects:

- a decrease of the gas density in $V_G$
- an increase of the flame velocity

The first effect would lead to a lower pressure peak because a decreased mass flow. The latter effect will lead to an increase of the max. pressure because an increased mass flow.
The density will vary proportionally to the temperature ratio. The flame velocity will increase as a function of the temperature ratio squared. So taking both effects in account one would theoretically expect an increase of max. pressure as a function of temperature.

#### 4.2.2.5 Test Facility

During the tests the combustion air was preheated with an electric air preheater with temperature control as indicated in figure 4.2.3.

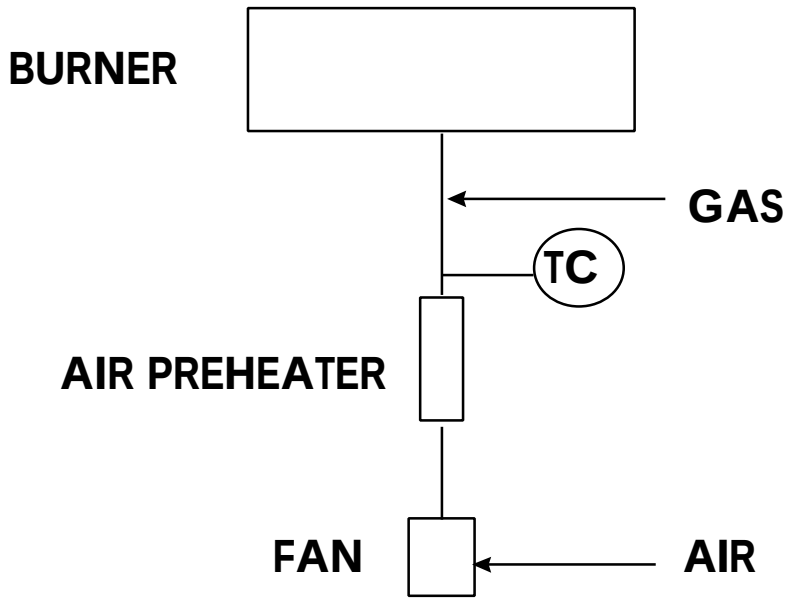


**Figure 4.2.3: Schematic drawing of the location of the air preheater.**

The temperatures mentioned are the temperatures of air leaving the preheater. Temperatures up to 500°C where reached. Although possible it was decided not to go higher to stay far from the self ignition temperature of the gas/air mixture. Gas was introduced downstream the electrical preheater for safety reasons. The gas to air ratio was controlled by a gas/air ratio controller which sets the gas pressure in a ratio to the measured air pressure. The air pressure was measured at the outlet of the fan. More details of the test facility are specified in the report of explosion tests ref [1].

### 4.2.3 Results

All the measurement results of the explosion tests performed are included in ref [1]. In the following text the results will be specified per subject.

#### 4.2.3.1 Design Rule

As the pressure levels are reasonably low in our case it is allowed to assume that f is not changing significantly as a function of the pressure levels. Keeping $f$ constant the design rule could be used to predict the reduction of the maximum pressure level in case the burner is filled with ceramic foam.
Based upon the reduction of $V_G$ and increase of $V_T$ one would expect the ratio Pfilled/Pempty to be 0.1.

| **Pfilled/Pempty** | |
|---|---|
| 0,07 | |
| 0,04 | |
| 0,08 | |
| 0,11 | |
| 0,04 | |
| 0,04 | |
| 0,04 | |
| 0,10 | |
| | |
| **mean** | **std** |
| 0,07 | 0,03 |

**Table 4.2.1: Statistics for the ratio of the measured $P_{filled}$ to $P_{empty}$.**

From the test results (table 4.2.1) it follows that the average value of the measured ratio P filled/P empty is 0.07.
Although the value is not equal to 0.1 the difference is not significant statistically.

#### 4.2.3.2 Safety Measure

The safety measure performed as expected. There were no explosions and the max. pressure level was reduced to a safe level. The ceramic foam was constructed of 3 larger pieces of 20 cm length and one smaller piece all pieces glued together. Visual inspection after the tests revealed that 3 long cracks in the ceramic foam were formed. See figure 4.2.4.

The one smaller piece of foam stayed intact. The cracks had no effect upon the effectiveness of the safety measure. The cracks are probably caused by a combination of thermal stress and pressure upsets. At high preheat temperatures the burner casing is thermally expanding this puts a stress upon the ceramics (glued to the structure).

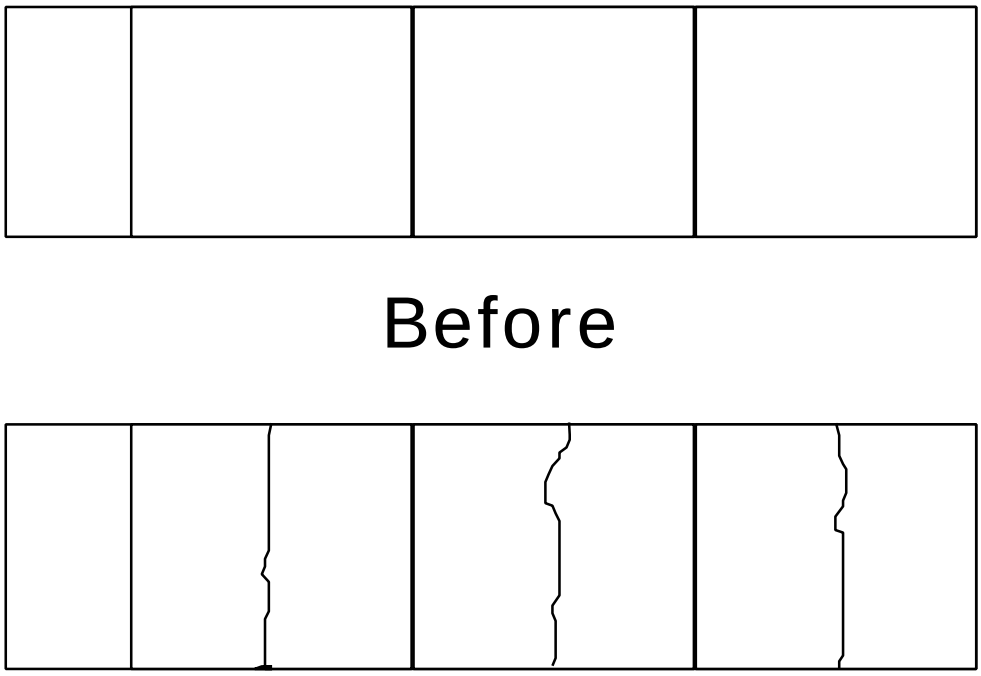


**Figure 4.2.4: Drawing showing the forming of cracks in the ceramic foam.**

During the test the burner was operated without a burner automatic. The burner automatic switches of the gas supply in case there is no flame detection signal. Because ignition below the burner deck occurred during the test the flame extinguished. As there was no burner automatic the gas supply stayed on. Because of this the gas starts burning at the surface of the ceramic foam (below the burner deck). Visual inspection after the test revealed that the perforated plate was buckled because of the burning below.
For normal operation a burner automatic is desired to protect the burner deck.

#### 4.2.3.3 Preheat Temperatures

As shown in figure 4.2.5 the measured Pmax initially goes up with preheat temperature as expected.
Until about 300°C the measured max. pressure rises with the preheat temperature. At higher temperatures the max. pressure starts to go down. This is caused by a lack of combustion air. At higher preheat temperatures the pressure head over the preheater and the system downstream the preheater is increasing because the higher velocity of the gas/air mixture. As the air-fan is kept at constant speed the air flow starts to fall down. Because the slightly rising air pressure the gas pressure is raised a little by the gas/air controller. So the air flow will decrease and the gas flow will increase a little. The gas / air ratio goes to the fuel-rich side. This will lead to a bad combustion with forming of CO and unburned hydrocarbons. As a result the temperature after the burner will decrease and less combustion gases are formed. Also the ignition below the burner deck will be less intense. This will cause lower max. pressure levels.

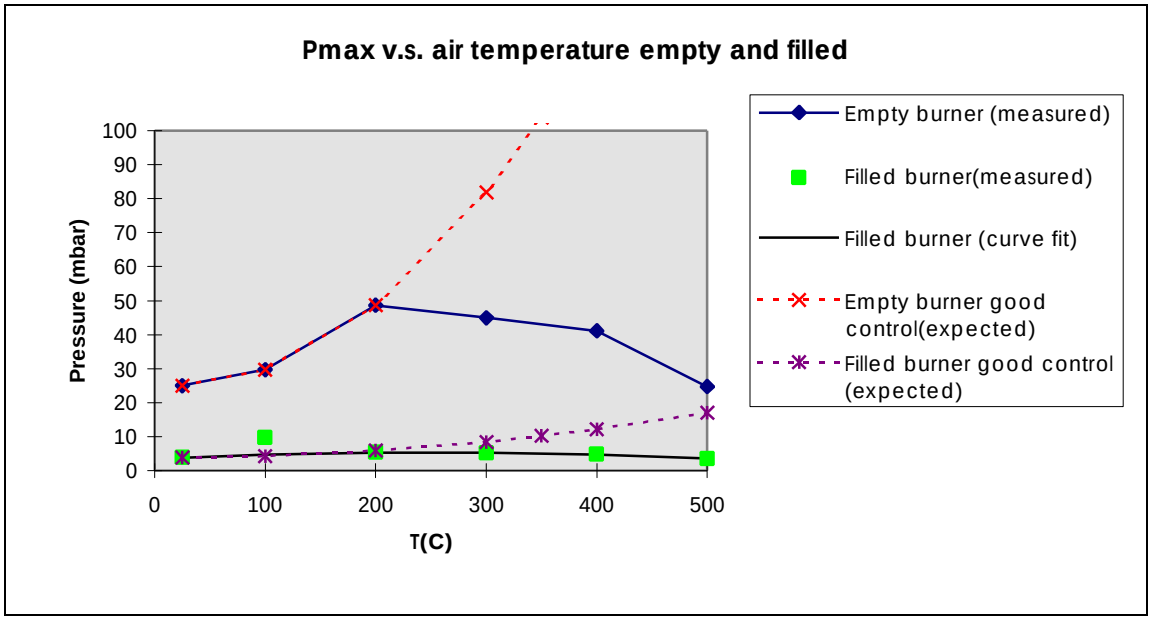


**Figure 4.2.5: Maximum pressure peak level as function of preheat temperature**

During the tests with higher preheat temperatures it was not possible to ignite the burner at max. capacity above 300°C preheat temperatures due to the offset in gas/air ratio. In figure 4.2.5 it is indicated what would be the expected pressure rises given a adequate gas to air ratio control. Without the safety measure above 300 °C the 100 mbar limit is exceeded. In a burner system equipped with a safety measure the max pressure levels are expected to stay well below the 100 mbar even for high preheat temperatures.

#### 4.2.3.4 Summary of the Main Results Achieved

The design rule is useful as a tool to predict the effect of the safety measure.

The safety measure is effective. A burner automatic is desired to protect the burner deck. A thinner layer of ceramic foam will probably function as well but the mechanical strength and thermal stresses require special attention.

Higher preheat temperatures cause higher max. pressures. This would lead to unacceptable pressure levels with an empty burner system if the gas/air ratio is maintained properly by more sophisticated control for preheat temperatures over 300°C.
For a burner system equipped with the safety measure the pressure levels although a bit higher will still be at an acceptable level even at high preheat temperatures.

## 4.3 Task 2, Development of the Premix Surface Burner

(Contractor: N.V. Acotech S.A., Belgium)

### 4.3.1 Introduction

This Task concerns the development of premix radiant surface burners, in which the burner surface is constructed from a metal fibre mat.

Two new and more economical types of metal fibre mats for burner surfaces have been developed by a new technology using coarser metal fibres. The matting technologies selected are sintering and knitting. Burners, made of samples resulting from the sintering and knitting technologies, have been submitted to an endurance test in which the most severe operational conditions were simulated (surface temperature 1000 $^{o}$C).

A new burner housing based on ceramic materials, able to withstand preheated combustion air up to several hundred degrees, has been designed. The burner housing has been equipped with the sintered and knitted mats selected. The concept of different combinations of housing/mat has been tested in a lab furnace to identify the best performing housing design.

Two premix radiant surface burners with two different mat materials and adapted housing design have been supplied for evaluation in Task 6 of the CECON-Programme.

This Task 2 has been divided in the following sub-tasks:

| **No** | **Sub-Task** |
|---|---|
| 2.1 | Development of an Economical Metal Fibre Burner Mat |
| 2.1.1 | Development of an Economical Sintered Fibre Mat with Coarser Metal Fibre |
| 2.1.2 | Development of a High-end Knitted Fibre Mat |
| 2.2. | Durability Testing of the Products Developed under Sub-task 2.1.1. |
| 2.3. | Development of a Two Specific Burner Housings Using a Sintered Metal Fibre and a Knitted Fibre Mat. |
| 2.4. | Durability Testing of 2 Combinations Housing/Material. |
| 2.5 | The Manufacturing of 2 Burners Selected on the Results of Previous Sub-tasks |

**Table 4.3.1: The sub-Tasks of Task 2 "Development of the Premix Surface Burner"**

### 4.3.2 Development of an Economical Metal Fibre Burner Mat

CONFIDENTIAL

### 4.3.3 Durability Testing of the Sintered and Knitted Metal Fibre Burner Mats

CONFIDENTIAL

### 4.3.4 Development of the Burner Housing

#### 4.3.4.1 General Requirements

A housing for an infrared radiant metal fibre burner working in a high-temperature environment should meet the following requirements :

* The housing should be temperature-resistant.
* Thermal expansion of the housing should not lead to deformation, leaks or gasketing failures.
* No part of the housing should reach a temperature level leading to potential danger for flashback.
* Combustion should be homogeneous controlled by the inlet tube or tubes and the distributor plate.
* Gas/air premix plenum should be as small as possible to reduce the risks in case of the unlikely event of a flashback.

#### 4.3.4.2 Burner for the Sintered Mat

The burner housing which has been developed is made out of a composition of ceramic materials. A construction ceramic resistant up to 500 $^{o}$C creates a gas confined housing on which the Metal Fibre Burner mat is fixed. The front and the side walls of the housing are covered with an insulating ceramic fibre layer resistant up to 1200 $^{o}$C. This ceramic insulation protects the box in such a way no part of it is exposed to a temperature exceeding 500 $^{o}$C.
The Metal Fibre Burner mat is fixed to the frame inside the box on the construction ceramic box. To control the thermal expansion of the burner mat, it has been segmented with ceramic paste into squares of maximum 100 x 100 mm. The intercrossings of the ceramic paste paths are fixed with specially shaped refractory steel buttons and steel wire to a structure of tubes underneath the fibre mat.
Segmentation and fixation limit the thermal expansion to the material locked in between the ceramic glue strips. The feeding tube has a 2" diameter and the free floating stainless steel distributor plate inside the ceramic housing has holes of 2 mm diameter with an open space of 3 %.

* Net MFB surface : 0.13 m$^2$.
* Firing conditions : 70 to 500 kW/m$^2$ in furnace condition between 500 and 800 $^{o}$C.
* Nominal output : 9.1 to 65 kW.
* Maximum operating surface temperature : 1050 $^{o}$C.
* Maximum surface peak temperature : 1100 $^{o}$C.
* Pressure drop : 20 - 100 Pa.

A prototype has been built for durability testing at Shell Recherche Grand-Couronne.
The Metal Fibre Burner mat used for the prototype was coded AC 200 P1.

#### 4.3.4.3 Burner for the Knitted Fibre Mat

The housing design is basically the same as defined in 4.3.4.2. Due to the elasticity of the knitted material there is no need to control thermal expansion. However, to cope with potential hang-outs we will have to use at some spots refractory steel buttons to fix the knitted material to the supporting stretch metal.
A prototype has been manufactured to be submitted to the durability test at Shell Recherche Grand-Couronne.

### 4.3.5 Durability Testing of 2 Combinations Housing/Mats

#### 4.3.5.1 Test Procedure

A furnace was built at Shell Recherche Grand-Couronne to perform a durability test on the prototypes developed under the paragraph 4.3.2. This furnace has the following characteristics :

* Dimensions : capable to hold the prototype burner as defined under the paragraphs 4.3.4.2 and 4.3.4.3.
* Temperature inside the furnace : 750 $^{o}$C.
* Cycling : 8 minutes on/2 minutes off - 24 hours per day.

#### 4.3.5.2 Prototypes and Results

The prototype with the sintered mat as defined under paragraph 4.3.2 was put to test in the furnace under the conditions as defined in 4.3.5.1 The test started in November '96 and lasted until the end of January 1997.

The prototype burner with the knitted mat was put under test from February '97 until June '97.

Both burners performed well. The excessive sagging effect of the downward radiating NIT burner asked for a better fixation design. An evaluation report on the ageing tests of the burners has been made by Shell Recherche Grand Couronne in France.

### 4.3.6 Manufacturing of 2 Prototype Burners for Evaluation in the CECON Programme

Two prototype burners with a net burner surface of 0.480 x 0.265 $m^2$ have been supplied to Gaz de France end of June '97.

One burner was equipped with the knitted mat, the other burner with the sintered mat.

The design of the burner with the knitted mat has been improved to avoid the sagging effect stated in the lab furnace at Shell Recherche Grand-Couronne.

### 4.3.7 Summary of the Main Results Achieved

1. A newly sintered more economical Metal Fibre Burner mat based on coarser metal fibre has been developed. It will not be industrialised because of unexpected high production investments needed for the manufacture of this mat.

2. A newly high-end knitted Metal Fibre mat was successfully developed and will be industrialised and put on the market place. The fact the product was performing well influenced the decision not to continue with the newly developed sintered mat.

3. The newly developed ceramic housing proves to work according expectation. Together with the knitted Metal Fibre Burner, it will be applied for gas radiant infrared applications in furnace conditions.

## 4.4 Task 3, Development of the Non-Premix Surface Burner

(Contractor: Danish Gas Technology Centre a/s, Denmark)

### 4.4.1 Introduction

The overall objective for DGC is, referring to ANNEX I in the EC-contract:

*Development of a non-premix radiant burner, that will be designed for high temperature conditions, i.e. high furnace temperatures (above 800°C) and high preheat temperatures (up to 700°C)( Task 3).*
The goal for the preheat temperature has later been changed to 1000°C.

The objective for the first project period is to make a study into materials suitable for the non-premix radiant burner (and choose the materials for the construction as well as to make proposals for the design of the non-premix radiant burner. The different proposals must be tested with a CFD-model (Computational Fluid Dynamics).
The objective of the second project period is to establish and test the developed prototypes for material deterioration, radiant efficiency, thermal load, excess-air interval, and emissions.
The two sub-activities have been individually reported in ref. [7] and ref. [8] respectively.

The overall conditions for the non-premix radiant burner are shown in figure 4.4.1.

The design activities have been based on the following burner parameters/restrictions:

| | |
|---|---|
| height x width: | ≤ 300mm x 300mm |
| fuel input: | 50 kW |
| combustion air temperature: | 800°C |
| furnace temperature: | 900°C |
| excess air: | 5% |

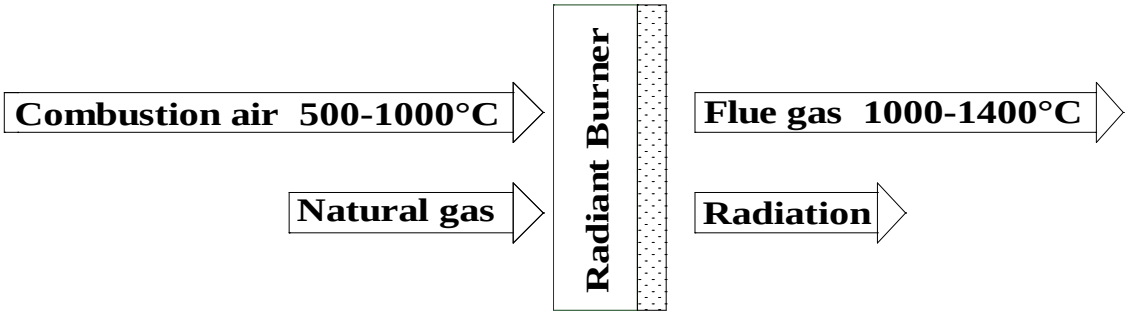


**Figure 4.4.1: The overall conditions for the non-premix radiant surface burner**

The specific load (550 kW/m$^2$) is very high and it has therefore been decided also to test the burners with smaller fuel input.

The restriction on burner dimensions has later been changed to:

height x width: ≤ 1000 mm x 1000 mm

This change makes it possible to construct a burner with a more suitable (lower) specific load than 550 kW/m$^2$.

### 4.4.2 Evaluation of Design Possibilities

The objective of the first project period was to:

- make a study into materials suitable for the non-premix radiant burner.
- choose the materials for the construction.
- make proposals for the design of the non-premix radiant burner.
- test the different proposals with a CFD-model.

In pursuit of finding a suitable material it is necessary first to estimate the maximum temperature that will occur in the burner. It has been estimated that the maximum adiabatic flame temperature will be about 2400 - 2500 K. The maximum temperature in the burner will of course never reach this level. A more realistic temperature was estimated to 2100 - 2300 K.
After finding a material that can resist these temperatures it is, knowing the material properties, possible to make numerical calculations that will determine a more precise maximum working temperature.

It has been noted that it is difficult to find data about material properties for ceramics in the mentioned temperature interval. After the literature study a few materials seemed promising. The final choice was made after having contacted some of the leading producers. It was possible to find one producer that could produce burners of one of the suggested materials, zirconia.

Several construction ideas for the non-premix radiant burner have been discussed and some of them tested with a CFD-model, ref. [9]. The proposed burner concept has been modified in order to obtain a

homogenous temperature distribution, enhance air and gas mixing and reduce the maximum material temperature.

The conditions for the CFD-calculations have been as follows:

| | |
|---|---|
| burner height x width: | 300 mm x 300 mm |
| fuel input: | 50 kW (specific load: 550 kW/m$^2$) |
| combustion air temperature: | 800°C |
| furnace temperature: | 900°C |
| excess air: | 5% |

Discussions and calculations have shown that the most promising way to distribute the gas in the burner is by using perforated ceramic tubes. The CFD-calculations have been based on ten tubes with an outer diameter of 10 mm, each perforated with 40 1 mm holes.

From the CFD-calculations it can be concluded that a cavity for mixing gas and hot air is necessary between two layers of ceramic foam. The concept is sketched in figure 4.4.2.

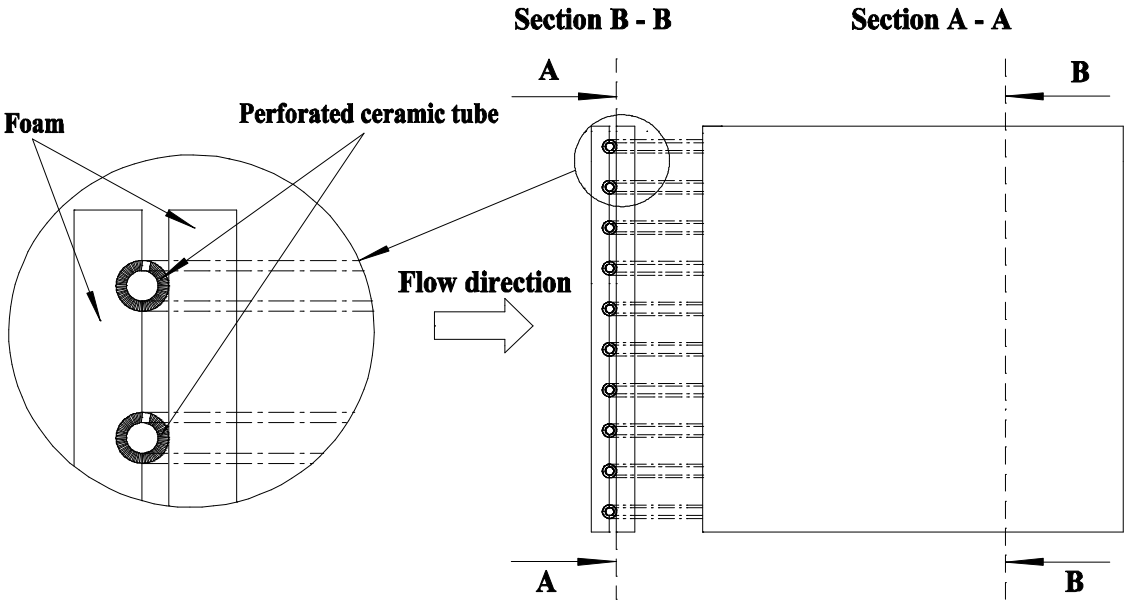


**Figure 4.4.2: Burner with grooves, tubes and a cavity inside.**

The height of this cavity in the direction of the bulk-flow should be not more than 5-6 mm. This small height prevents the gases to react completely, and therefore the temperature is kept at an acceptable level.

From the CFD-calculations it can also be concluded that the distance between the gas jets can be increased while the diameter of the jets should be decreased. A suggestion could be a distance of 20 mm instead of 15 mm and a diameter of 0.8 mm instead of 1 mm. This would double the velocity of the gas in the jets and enhance mixing between the gas and the hot air bulk flow.

From the CFD calculations it can be seen that a large amount of unburned fuel will leave the surface of the burner. As an option, it was suggested to add extra ceramic foam to the construction sketched in figure 4.4.2 to increase the burnout of the fuel in the burner. This layer should have a much larger poresize giving much better radiation conditions and a better opportunity for the gases to burn out. This idea is outlined in figure 4.4.3. Eventually, the prototype was constructed without the extra foam in order to simplify the validation of the basic burner design.

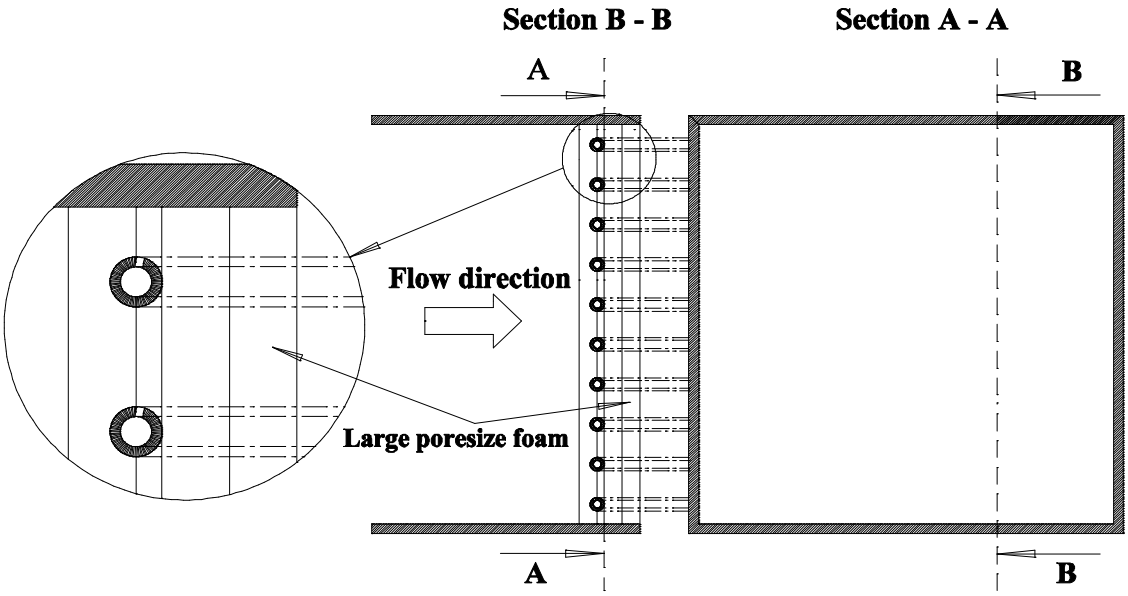


**Figure 4.4.3: Sketch of prototype number 1.**

Another idea for a prototype was found at the Netherlands Energy Research Foundation (ECN), see figure 4.4.4.
This construction could be characterised as consisting of two burners, an “inlet burner” and an “outlet burner”. The flue gases from the “inlet burner” surface are sucked out through a ceramic foam of the “outlet burner” in which burnout of unburned gases can be ensured.

This concept has been developed for traditional surface burners to reduce flue gas losses and increase the effective radiant surface area. The ceramic foam of the outlet section is heated by the flue gasses and will obtain a temperature not much lower than this. The irradiation from this surface will increase the radiant efficiency of the system and this effect will be even more significant at high flue gas temperatures and combustible components in the flue gas.

The two non-premix radiant burner prototypes constructed and tested are based on the concepts illustrated in figure 4.4.3 and figure 4.4.4.

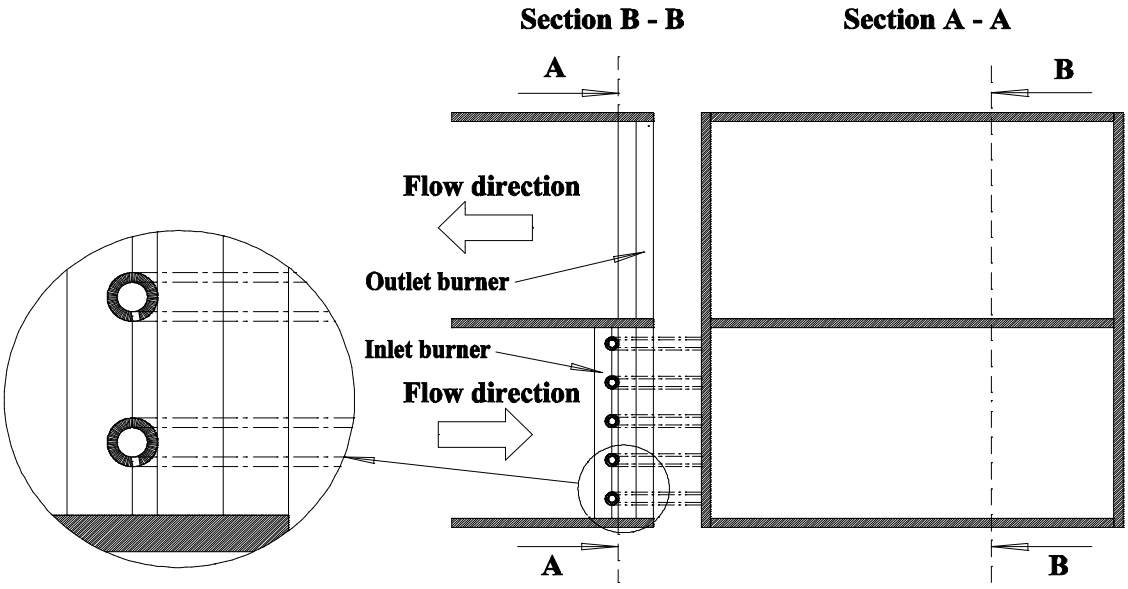


**Figure 4.4.4: Sketch of prototype number 2.**

The calculations of the temperature in the burner sketched in figure 4.4.2 give a maximum of approximately 1730°C. This means that the chosen material, ziconia, can be used for the foams. As described in chapter 4.4.3, another material was eventually chosen for the prototypes.

After the initiation of the project the goal for the non-premix radiant burner has been changed. The combustion air preheat temperature has been raised from 800°C to 1000°C. Also the geometrical restrictions has been changed from 300 mm x 300 mm (width x height) to 1000 mm x 1000 mm. However, the qualitatively result of the design evaluation provides sufficient information for the implementation of these changed design parameters into the prototype construction. The prototypes will be constructed with a height of 300 mm and a width of 400 mm. These restrictions are made because of the shape of the test furnace in DGC's own laboratory.

### 4.4.3 Experimental Results

The objective of the second project period is to construct and test the prototypes designed in the first project period for material deterioration, the process efficiency, the thermal load, the excess-air interval, and the emissions.
The prototypes have been constructed on the basis of the concepts found in the first project period, as shown in figure 4.4.5.

Some practical changes have been made to make the construction simpler and cheaper. The groves in the upstream foam sections have been left out in the final construction, as it has been estimated that the influence on e.g. flow patterns is small. At the end of the first project period it was suggested to add an extra layer of ceramic foam on the furnace side of the burner to ensure burn-out of the gas. This extra layer of foam has not been used because it would also complicate the construction. Figure 4.4.6 shows the outline of the constructed burners.

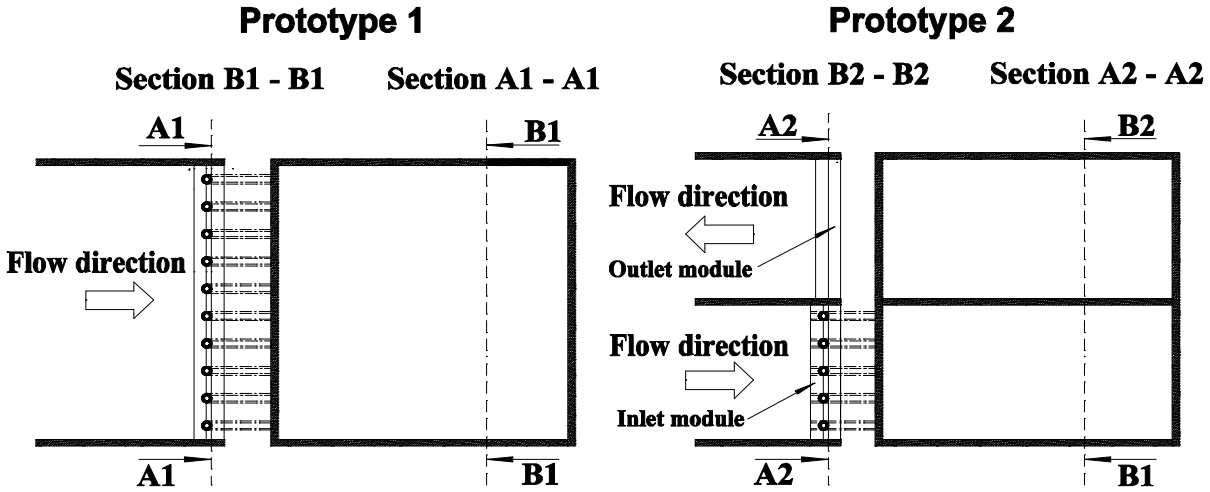


**Figure 4.4.5: Sketch of the two concepts for the non-premix radiant burner found in the first project period.**

During the design phase, ziconia was chosen as the preferred burner material. It is possible to produce foams of this material, but the price of these prohibited that it was used for the prototype construction. The temperature distribution and thermal stresses of the burners has been thoroughly discussed with the burner supplier, ECO Ceramics. Eventually, the material "x-mullite" was chosen for the prototypes, which is a modified mullite-based material provided by ECO Ceramics.

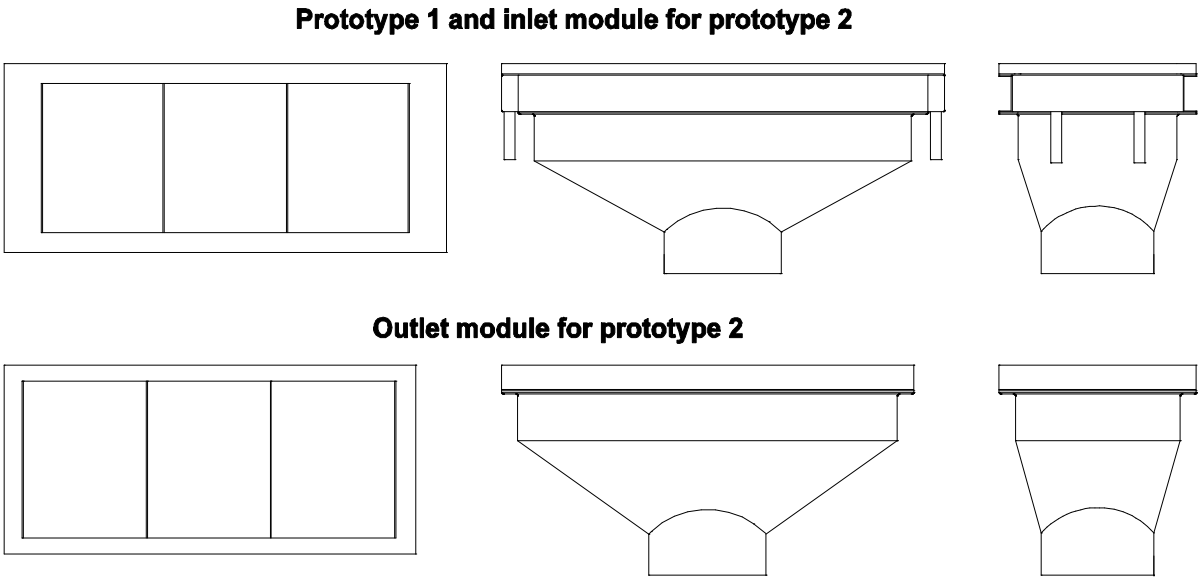


**Figure 4.4.6: Outline of prototype 1, which also is the inlet burner in prototype 2, and outline of the outlet module in prototype 2.**

The prototypes were planned to be tested in a water-cooled furnace (the SERB test furnace, ref [10] and in a high-temperature furnace (ceramic furnace). The SERB test furnace provides possibilities for making performance tests (heating experiments using a metal plate), where the ceramic furnace only provides possibilities to test the behaviour of the burners in high-temperature conditions.
The performance tests were planned to be for determining the optimum working condition for the prototypes with different preheated combustion-air temperatures. Also tests of off-design conditions were planned. In the high-temperature furnace it was decided to determine burner surface temperature, emissions and which temperature profile the burners would create in the furnace.
The initial experiments were performed with low combustion-air preheat-temperatures, approximately 450°C, in which case the combustion took place on the outer surface of the downstream foam. The distribution and the mixing of gas and air was poor, and the temperature distribution was very unhomogeneous. From the amount of CO and $C_XH_Y$ in the flue gas it was also concluded that the burner was not working very good. Further experiments with a higher specific load with the same combustion-air preheat-temperature gave the same distribution problems.

The next step in the series of planned experiments was to raise the combustion-air preheat-temperature to 600°C. When the combustion-air preheat-temperature reached nearly 600°C the burner surface emitted visible radiation and the combustion zone moved into the cavity between the upstream and downstream foam sections. A deposition of soot started on the surface of the downstream foam a few minutes later. The deposition increased and eventually covered about two thirds of the burner surface, mainly at the two outermost foam sections, see figure 4.4.7.

There was no indication that the deposited soot would disappear. It was attempted to change both the excess-air ratio and heat input, but the soot deposition could not be avoided. When the gas supply was disconnected the deposited soot slowly burned and a large part of deposited soot disappeared.

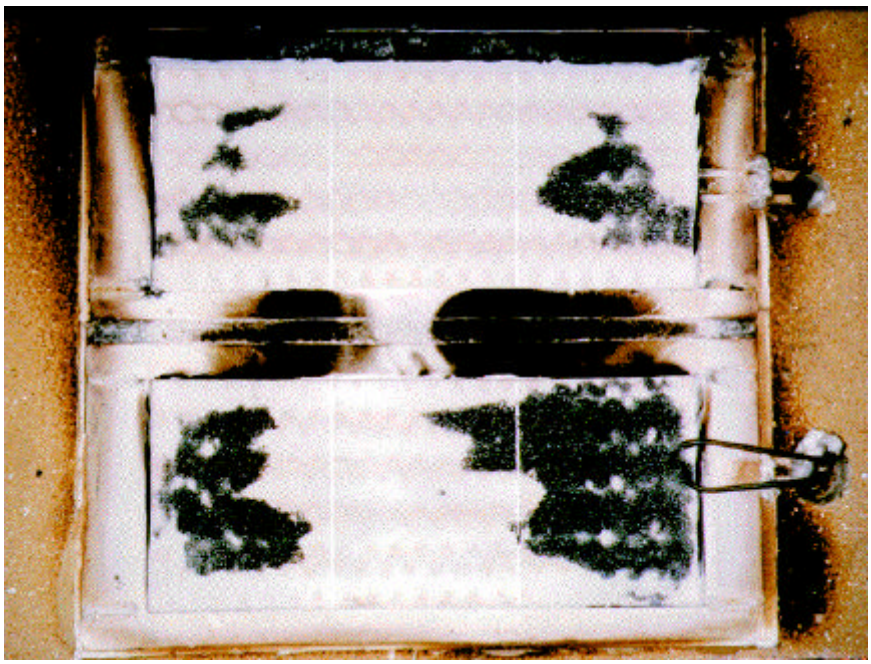

**Figure 4.4.7: Picture of the front of the burners after the formation of the dark areas.**

An inspection of one of the burners also revealed deposition of soot on the back of the downstream foam sections. The inspection also revealed that the ceramic tubes were partly blocked by soot in the middle section.

The small cavity of 13 mm between the upstream and downstream foam sections was changed to 150 mm. The purpose was to increase the distance between the combustion zone and the surface of the ceramic tubes and thereby lower the temperature on and inside the tube. If cracking of the gas was avoided inside the tubes, it was possible that any soot particles would manage to burn out before reaching the downstream foam sections. Unfortunately, the result was the same as described above, and the conclusion after having tried testing prototype 1, which also should have operated as an inlet burner in prototype 2, was that the designed burner cannot be utilised without major modifi- cations.

It was impossible to conduct a totally new design process due to the time schedule and financial situation of the project. However, in order to demonstrate the concept of a non-premix radiant burner, a test burner, prototype 3, based on a new and simpler construction was established, see figure 4.4.8.

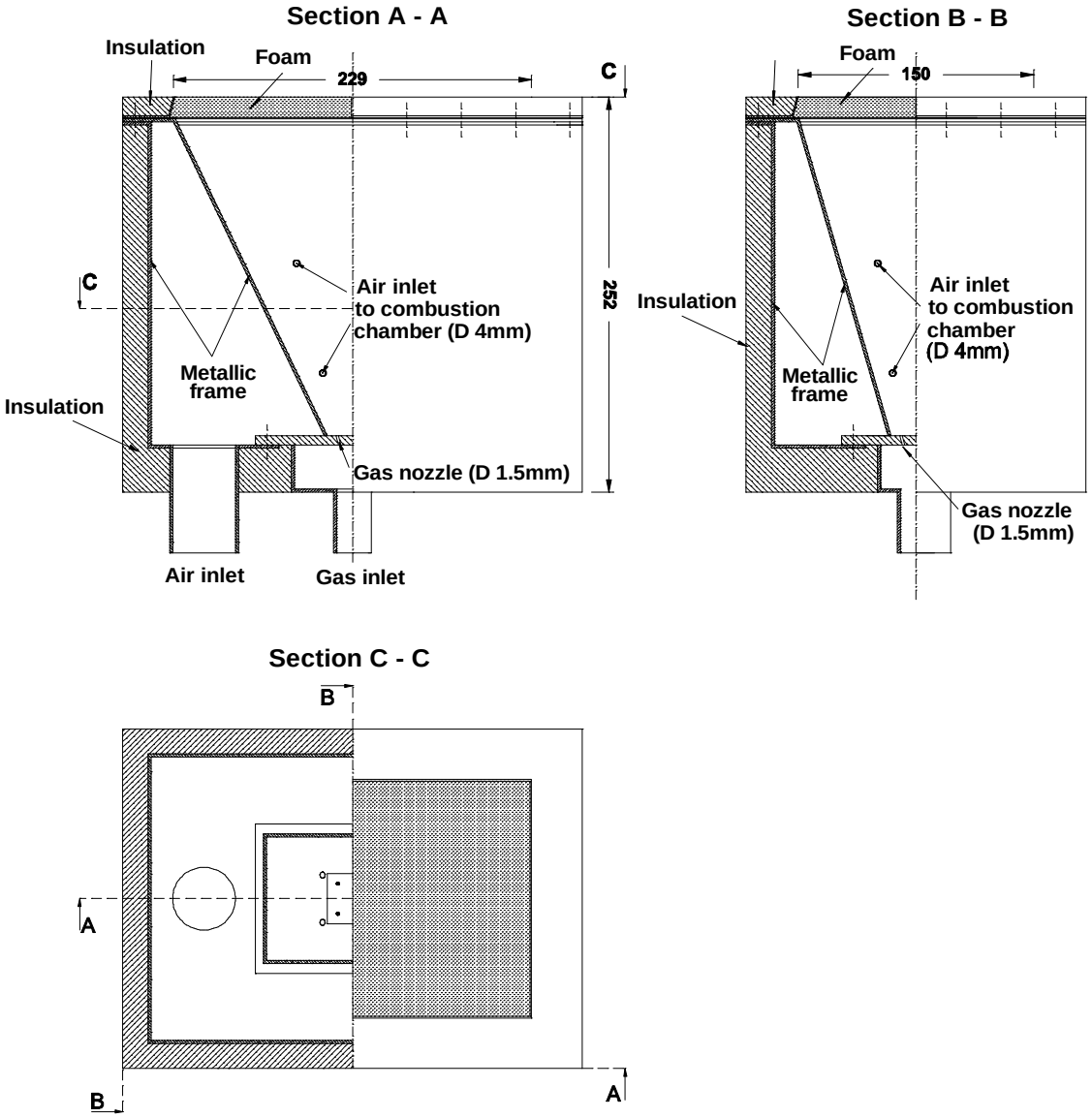


**Figure 4.4.8: Sketch of design of prototype 3**.

In this burner the gas is injected through four holes in the bottom of the burner. This means that the gas is not preheated before it enters the combustion chamber. The combustion air is supplied through eight

holes, two in each side of the combustion chamber. The position of these inlets creates a highly swirling flow which insures good mixing of air and gas. The combustion chamber was built in stainless steel, which of course is only capable to withstand the high temperatures for a short period of time. However, the prototype 3 burner demonstrated that the construction worked, and it was decided to construct a high-temperature-resistant prototype in order to test the concept further.

The combustion chamber of prototype 4 was built in ceramic stone which could withstand the high temperatures. However, the steel frame which fixates the foam sections broke down after only a few experiments. This part of the burner was improved in prototype 5, and with this burner it was possible to carry out two series of experiments. A sketch of the prototype 5 burner is shown in figure 4.4.9.

Three measurements were carried out without preheating of the combustion air, with specific loads between 240 kW/m$^2$ and 450 kW/m$^2$. Then the combustion air was preheated to approximately 400°C, and the process efficiency was measured at specific loads from 230 kW/m$^2$ to 475 kW/m$^2$.

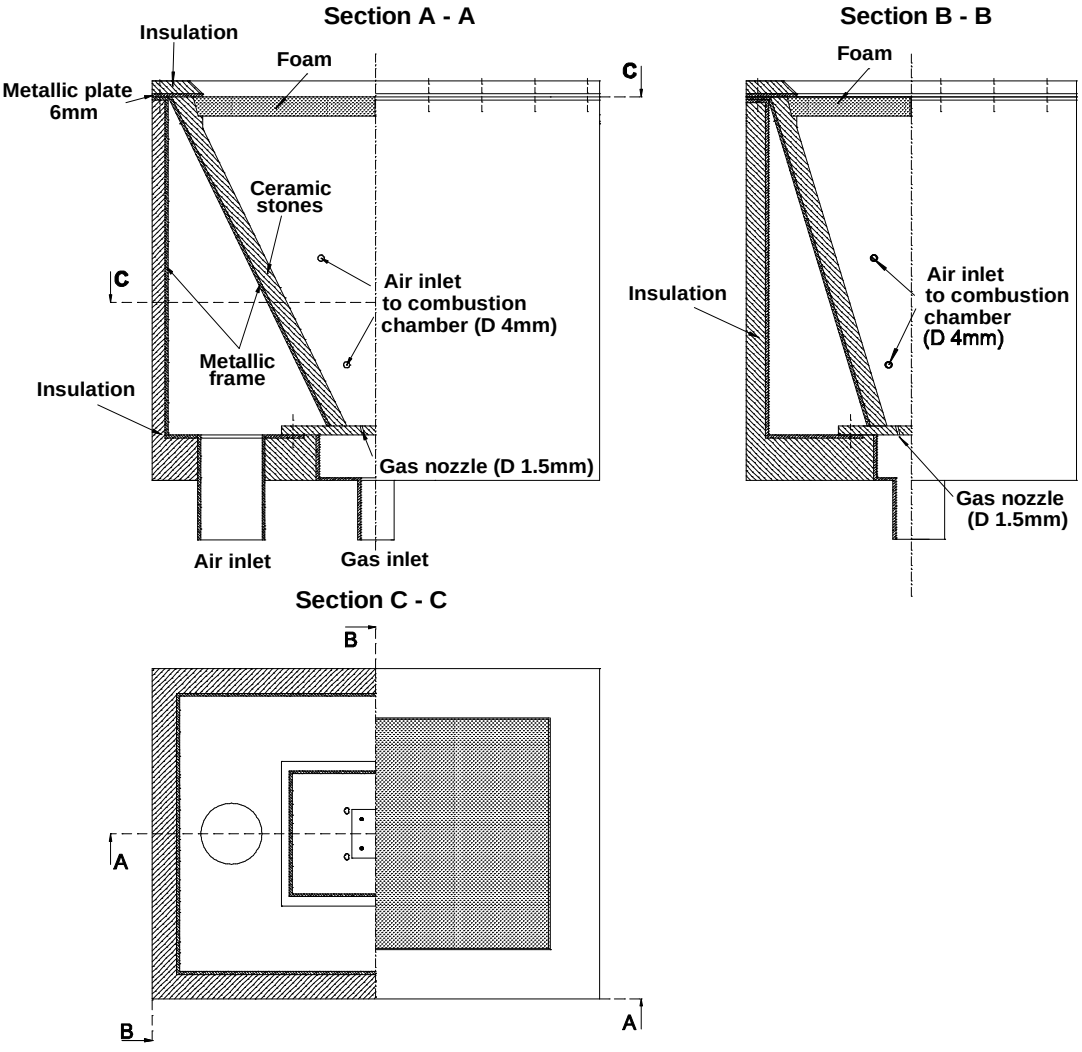


**Figure 4.4.9: Sketch of design of prototype 5**

Eventually, the ceramic foam sections could not withstand the operating conditions: Both of the two foam sections that make up the burner surface curved outwards. A crack in one of the foam sections,

which did not influence the burner operation during the initial tests, grew and finally the section opened completely.

The measured process efficiencies are shown in figure 4.4.10. They are compared with results from previous experiments with four different surface burners, ref [11].

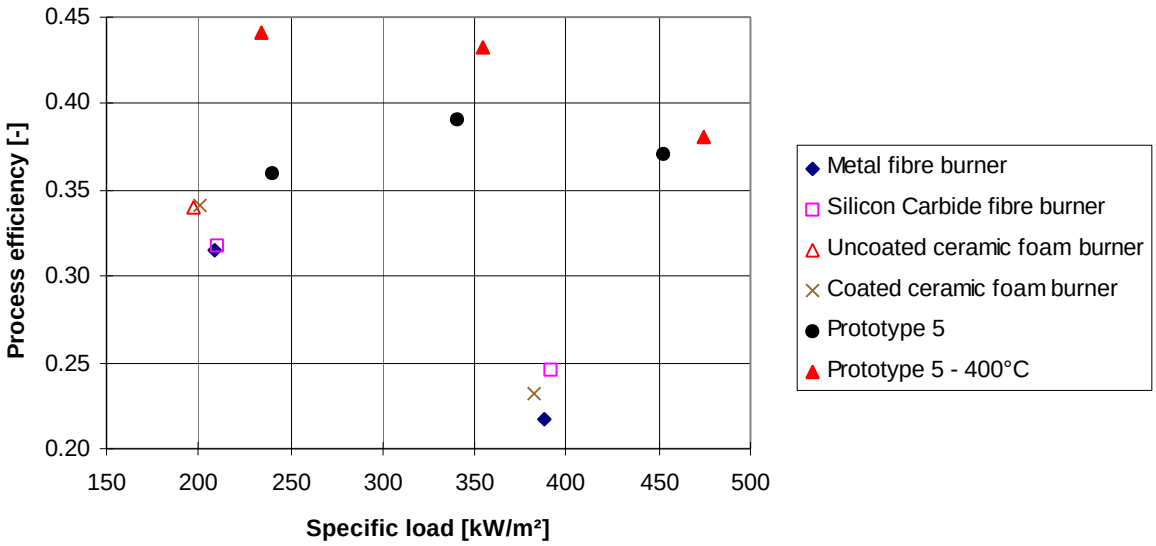


**Figure 4.4.10: Measured process efficiencies with prototype 5 and reference data from previous experiments.**

The results without combustion-air preheating are superior to the reference data, especially at high loads. This is explained by the fact that prototype 5 is not a surface burner. At low loads the radiant efficiency of surface burners increases with the heat input. However, when the load exceeds a certain optimum, the radiant efficiency decreases because a significant amount of the supplied gas leaves the burner before it is burned. At extreme loads the combustion will turn into a blue flame mode where the entire combustion takes place downstream of the burner. This effect is not observed
for prototype 5 since the combustion zone in this burner is not fixed at the surface of the foam sections.

Figure 4.4.11 and figure 4.4.12 show the measured emissions without and with combustion-air preheating respectively.

The $NO_X$-emissions increase with specific load and with the temperature of the combustion air. Preheating the combustion air to 400°C has a much larger effect on the $NO_X$-emissions than an increase of the specific load from approximately 240 kW/m$^2$ to 450 kW/m$^2$. Without preheating, $NO_X$-levels (corrected to zero oxygen content) between 170 ppm and 390 ppm were observed, while 330-1050 ppm $NO_X$ was measured with combustion-air temperatures of 400°C.

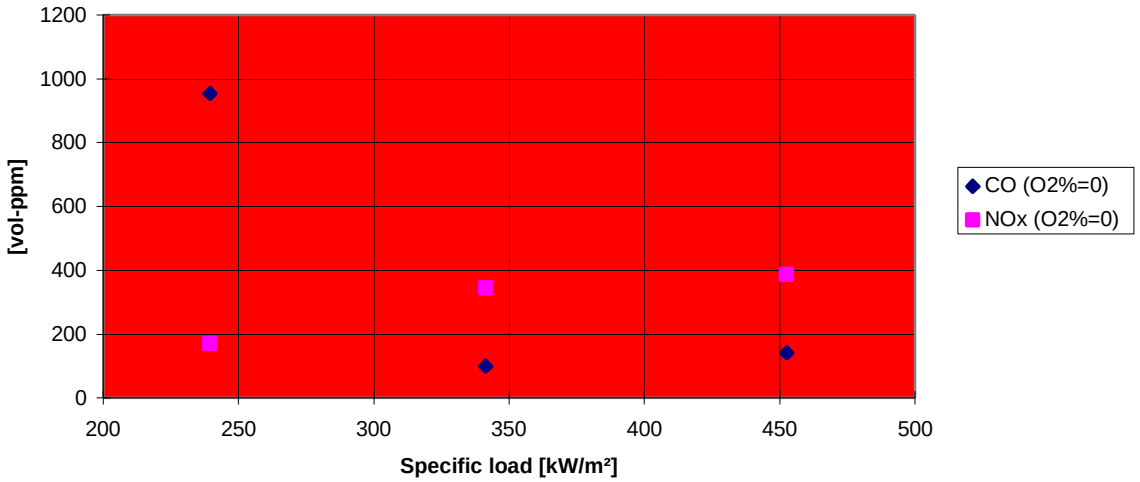


**Figure 4.4.11: Emissions of CO and $NO_X$ corrected to 0% $O_2$ from the prototype 5 burner without preheated combustion air.**

Besides one unexplainable high measured CO-content of approximately 950 ppm (corrected to zero oxygen content), the CO-emissions without preheating were between 100 ppm and 140 ppm. When the combustion air was preheated to 400°C, the emissions reached a level between 240 ppm and 510 ppm.
The experimental results can be summarised in the following conclusions:

The developed prototypes cannot be operated with combustion air preheated to 400°C or higher.
A relative improvement of the process efficiency by 22% has been observed when the combustion air is preheated to 400°C.
The $NO_X$-emissions increase significantly and much more than the process efficiency when the combustion air is preheated.
The process efficiency obtained with prototype 5 is better than previously investigated surface burners, especially at high loads.

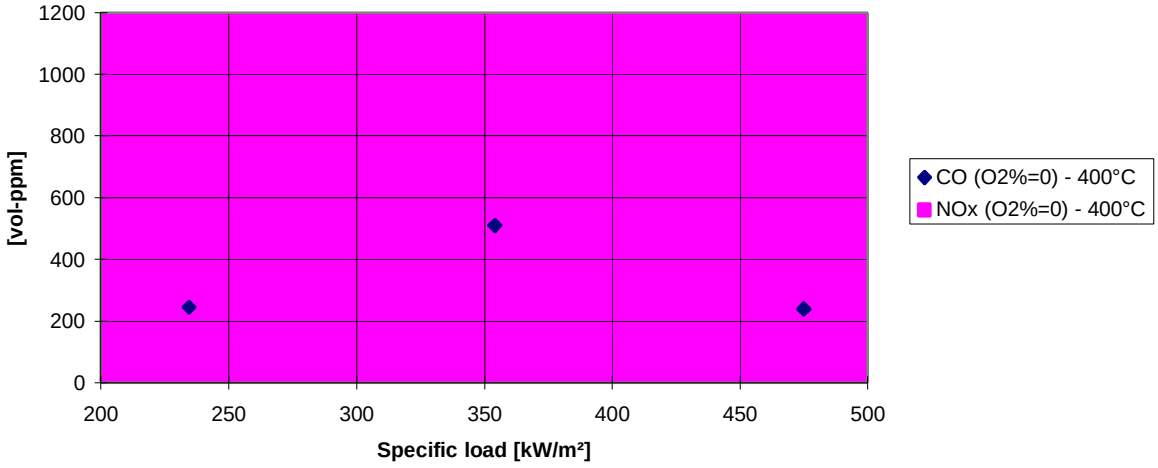


**Figure 4.4.12: Emissions of CO and $NO_X$ corrected to 0% $O_2$ from the prototype 5 burner with combustion air preheated to 400°C.**

### 4.4.4 Summary of the Results Obtained

The objective of Task 3 of the CECON project was to develop and test a non-premix radiant burner. An investigation has been conducted on feasible materials for production of porous burner foams and the thermal properties of these materials.

A burner concept, prototype 1, was developed with special attention to minimise emissions and foam peak-temperatures. A central problem in this context is to obtain the highest possible homogeneity of the combustion, which means that gas/air mixing should be optimised. In order to fulfil this, prototype 1 was designed with ceramic gas distribution tubes perforated with small holes. The design was supported by numerical simulation of flow, combustion and radiation of the burner with the CFD-code TUFCA.

During the test of the prototype it became evident that the construction was not feasible, because the ceramic gas distribution tubes eventually were blocked by soot. Experiments to investigate if the gas would crack conducted prior to the construction of the burner did not indicate that any problems would occur. It can therefore be concluded that the experiments did not simulate burner conditions adequately.

In order to identify possible modifications to avoid this, the gas temperature profile in the tubes has been evaluated. The gas temperature rises to the temperature of the outer surface of the tube almost immediately after entering the tube from the manifolds on both sides of the burner. Compared to the cracking test which was carried out prior to the construction of the burner, the residence time at the final (high) temperature in the real burner tube is much lower. This means that, as far as residence time is concerned, the test was conservative. An explanation of the fact that the gas cracked in the burner tubes, and not in the test, can be that the tube temperature in the test was too low to simulate burner conditions.

The outlet temperature of the gas when it leaves the distribution tubes can theoretically be modified by changing parameters as tube (inner) diameter as well as the number and diameter of the holes in the distribution tubes. However, the ratio of the inlet area to the tubes and outlet area through the holes cannot be changed without compromising the homogeneity of the gas distribution. Therefore, it is not believed that the problem can be solved by simply using other tube configurations. A possible, but complicated, solution is to cool the gas through the tube e.g. with air or water. The cooling could be established in a solution with concentric tubes, in which the inner tube contains the cooling medium.

Alternative prototypes in which the gas is not heated prior to injection into the combustion chamber have been established. The concept operated satisfactorily without preheating of the combustion air, although $NO_X$-emissions were high. The measured process efficiencies were superior to previous results for different kinds of premix surface burners. When the combustion air was preheated to 400°C, the foam sections broke down.

Possible means to improve durability, efficiency and emission level for both burner concepts have been suggested but not tested. These include cooling of the gas in prototype 1, coating of the downstream side of the foam section to improve the radiant efficiency and multistep combustion.

## 4.5 Task 4, Modelling of the Ceramic Heat Exchanger

(Contractor: Katholieke Universiteit Leuven, Belgium)

### 4.5.1 Introduction

The second sub-objective of the CECON-project concerned the development of a ceramic heat exchanger capable of achieving high levels of heat recovery.

Two kinds of activities can be distinguished in this Task:

1 Experiments on the pressure drop on finned surface flow passages; the information gathered is used to improve the heat exchanger-model.

2 Activities on the design of the heat exchangers used in the Tasks 5 and 6 of the project, as well as the verification of the predicted characteristics afterwards.

### 4.5.2 The Use of Thick Fin Heat Exchanger Surfaces in Flue Gas Recuperators

This section describes the results of an experimental investigation of the pressure drop for air flow through thick fin heat exchanger passages. Thick fin surfaces are common in flue gas heat exchangers such as cast iron air preheaters and high temperature silicon carbide flue gas heat recovery systems. The fins typically measure 10 to 40 mm in height, 40 to 100 mm in length, and 3 to 5 mm in thickness. They are aligned in the direction parallel to the flow, can be staggered or aligned relative to each other, and provide flow passages with hydraulic diameters of the order of 10 to 20 mm. The surface density is of the order of 200 $m^2/m^3$. Premium casting technologies are needed to produce high densities with a minimum of material. This section presents the results of pressure drop experiments of air flow through a set of thick fin flow passages with different dimensions and fin shapes.

The nomenclature and design and computation procedures are taken from the literature. Kays and London (ref [12]), Kakac, Shah and Aung (ref [13]) and Van den Bulck (ref [14]) give all the information necessary to correctly use the information provided in this document.

#### 4.5.2.1 The Experimental Set-up

The experimental rig consists of an entrance section, a test core, an orifice plate and a curved blade fan. Figure 4.5.1 shows the flow scheme. Laboratory air is drawn through the entrance section which provides a smooth, straight flow. The contraction ratio is 8 to 1. Metal screens at the end of the contraction provide reproducible, small scale turbulence upstream of the test section.

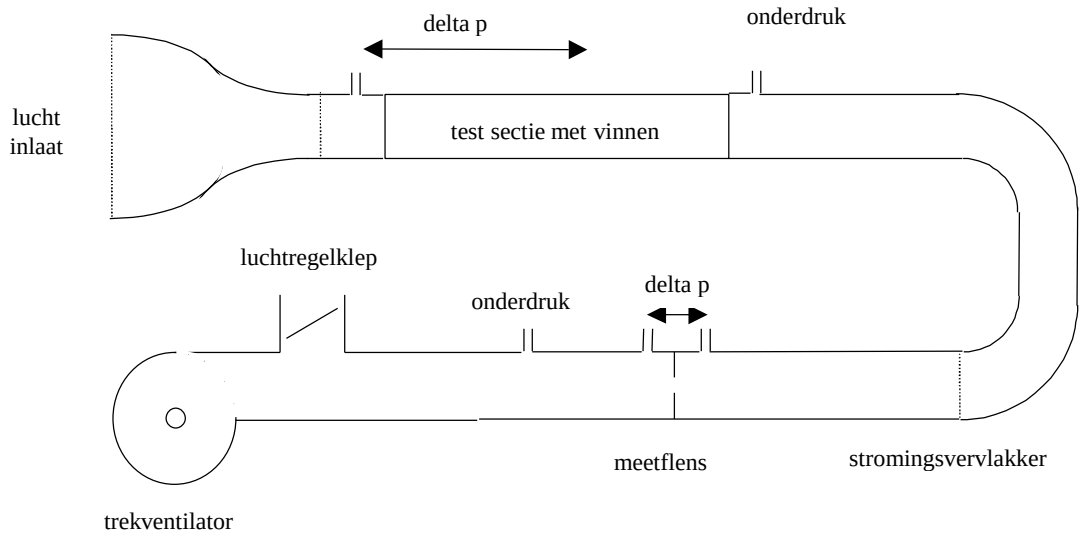


**Figure 4.5.1: Schematic overview of experimental rig.**

Downstream of the test section are a honey-comb flow straightening device, another metal screen and an orifice plate for flow rate measurements. Pressure drops across the test section and the orifice plate are measured with U-tube manometers. Four pressure tappings are distributed along the perimeter of the duct and are mounted in parallel to feed the manometers. The accuracy of the U-tube readings is ± 0.5 mmWC on an average pressure drop of 100 mmWC for the test section and ± 0.01 mmWC on an average pressure drop of 10 mmWC for the orifice plate, respectively. In addition, the overall pressure difference between the flow downstream of the orifice plate and the laboratory room is measured with a U-tube similar to the one that is used for the test section. This measurement provides redundancy, and the accuracy of the pressure drop recordings is improved by using a 'data reconciliation' procedure. Flow rates are measured with an orifice plate that is designed according to current standards.

#### 4.5.2.2 Data Reduction

The pressure drop for isothermal flow through a heat exchanger flow passage can be written as:

$$\Delta P = \left( K + f \frac{4L}{D_h} \right) \frac{(\rho V)^2}{2\rho}$$

in which the mass flux ($\rho V$) is computed from

$$\rho V = \frac{m}{A_c}$$

in which $m$ is the mass flow rate through the core passage.

The geometry of the heat exchanger core passage is described by four parameters of which three are independent of each other. These geometrical parameters are:

| | | | | |
|---|---|---|---|---|
| 1. | The heat exchanger core passage minimal free flow area | | $A_c$. | $m^2$ |
| 2. | The heat exchanger core passage exchange surface area | | $A$ | $m^2$ |
| 3. | The heat exchanger core passage flow length | $L$ | m | |
| 4. | The heat exchanger core passage hydraulic diameter | $D_h$ | m | |

The hydraulic diameter $D_h$ is computed from the first three parameters by:

$$D_h = 4\ A_c\ L\ /\ A$$

The pressure drop coefficient $K$ is the sum of the entrance and exit losses. For isothermal flow, these end losses can be correlated as:

$$K = K_c + K_e \quad \text{where} \quad K_c = 0.4(1-\sigma^2) + a\ Re^{-0.25} \quad \text{and} \quad K_e = (1-\sigma)^2 - a\ \sigma\ Re^{-0.25}$$

where $\sigma$ is the entrance flow area contraction or exit flow area expansion. The coefficient $a$ is dependent upon the geometry of the flow passages and for the finned surfaces that are the subject of this investigation, $a$ = 1.1. The Reynolds number that appears in the formulas is computed upstream of the port.

The parameter $f$ in the pressure drop equation is the (Fanning) friction factor. For a given flow passage, this parameter is a function of only the Reynolds number of the flow within the flow passage: $Re = (\rho\ V)\ D_h\ /\ \mu$. The interdependence of the friction factor and the Reynolds number is unique for every flow passage, and for every complicated finned surface flow passage, needs to be determined experimentally.

#### 4.5.2.3 Description of Heat Exchanger Surface and Test Cells

The test section of the experimental rig contains a finned surface heat exchanger flow passage. The flow passage is constructed from two cast iron finned plates that are mounted face-to-face in a rectangular duct. One plate rests on the bottom of the rectangular duct and faces upwards. The other plate faces downwards and is mounted on a carrier board that can be moved up or down. The spacing between the fin tips of the opposing plates can thus be varied continuously by lifting the top plate. The test section is configured to assure that the air flows through the finned passage and is sealed on the outside with an adhesive tape.

Two types of finned surfaces have been examined. Type I has fins that are aligned one after the other. Type II has fins that are staggered. The fins have a tapered cross section. The geometrical properties of both surfaces are listed in table 4.5.1 and are compared to the finned surface of the Schunk elements that are used in the CECON heat exchanger.

| **Geometrical property** | | **Type I** | **Type II** | **Schunk** |
|---|---|---|---|---|

| | | | | (internal) |
|---|---|---|---|---|
| Fin surface roughness (mm) | | 0.30-0.35 | 0.30-0.35 | |
| Fin length (average) | mm | 48.0 | 38.0 | 35.0 |
| Fin height | mm | 33.0 | 30.0 | 15.0 |
| Fin thickness (bottom) | mm | 4.5 | 4.5 | 4. 04 |
| Fin thickness (top) | mm | 1.5 | 2.0 | 3.04 |
| Fin pitch (parallel/longitudinal) | mm | 12.6/55.0 | 14.0/45.0 | 7.72/45.0 |
| Clearance between fin tips, *h* | mm | 5.0-25.0 | 0.0 - 25.0 | |
| Number of fins (two sides) | | 640 | 664 | 48 |
| Free flow area, $A_c$ | $cm^2$ | 60-91 | 55-86 | 27.4-110.7 |
| Friction exchange area, *A* | $m^2$ | 2.56-2.65 | 2.07 - 2.15 | 0.00637 |
| Test plate length, *L* | m | 1.713 | 1.638 | 45.0 |
| Hydraulic diameter, $D_h$ | mm | 15.9-23.6 | 17.4 - 26.2 | 6.10-30.03 |

**Table 4.5.1: The geometrical properties of the experimental rig and of the finned surface of the Schunk elements that are used in the CECON heat exchanger.**

#### 4.5.2.4 Experimental Results

Pressure drops versus flow rates are recorded for surfaces type I and type II for varying distance between the fin tips. The pressure drop is converted into the friction factor *f* and the mass flow rate is converted into the Reynolds number, *Re*. The formulas for these conversions are given above.

Figure 4.5.2 shows the experimental results for the type I flow passage. The friction factor decreases asymptotically with increasing Reynolds number. For a small spacing between the fin tips, the friction-factor/Reynolds-number correlation compares well with that for a cylindrical duct with equal hydraulic diameter and a surface roughness equal to that of the fin surface (cast iron, 0.35 mm). This means that the fact that the fins are interrupted in the flow direction does not change the hydraulic characteristics of the flow passage. The passage behaves as if the fins were continuous strips with the same exchange area as the passage with individual fins. This experimental finding is very important, because existing correlations for cylindrical ducts can be used within the typical range of accuracy that is offered by these correlations.

Figure 4.5.2 also shows the variation of the friction-factor/Reynolds-number correlation with fin tip spacing. The experimental data clearly show that the friction factor decreases with increasing fin spacing. The table 4.5.2 lists the asymptotic value for large Reynolds numbers, $f_\infty$, also known as the friction factor for fully developed turbulence.

.

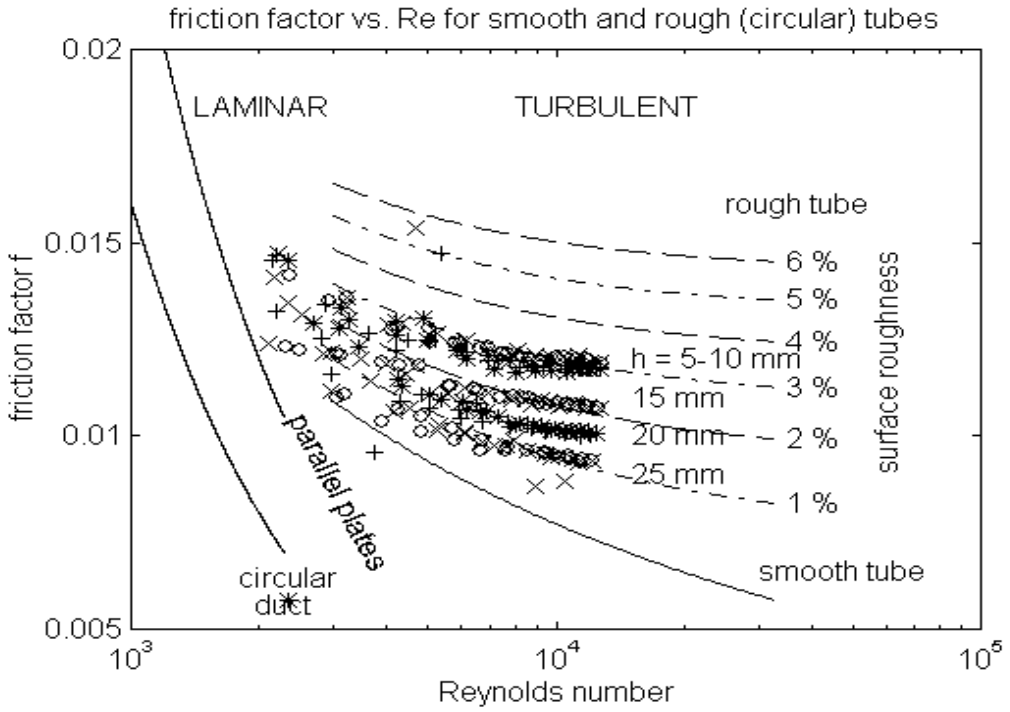


.

**Figure 4.5.2: Experimental results type I non-staggered fins. (h is the fin tip clearance).**

These data reveal that for a spacing between the fin tips which is of the order of the hydraulic diameter, the friction factor may be reduced by as much as 16 %. This reduction in friction factor, which manifests itself for the full range of the Reynolds number, is actually reflective of a reduction of the frictional surface area. By enlarging the fin tip spacing, the air flows progressively more through the free space that is created between the opposing fin tips in the middle of the channel. The velocity along the fin side surfaces, and thus in between parallel fins, is reduced. The recommendation for finned surface flow passages is that the free flow area should be created by adjusting the fin pitch, i.e., the spacing between parallel fins. The opposing surface should 'touch' the fin tips. The figure 4.5.3 illustrates this principle. Two flow passages with the same free flow area are show. The flow passage on the right is better because the flow area is provided between the parallel fins and will offer a larger surface exchange area for friction and consequently also for heat transfer.

| Fin tip spacing, h (mm) | Friction factor (Re® ¥), $f_{¥}$ |
|---|---|
| 0 | 0.0118 |
| 5 | 0.0117 |
| 10 | 0.0115 |
| 15 | 0.0106 |
| 20 | 0.0099 |
| 25 | 0.0093 |

**Table 4.5.2: The asymptotic value for large Reynolds numbers $f_{¥}$, (the friction factor for fully developed turbulence) as function of the fin tip spacing.**

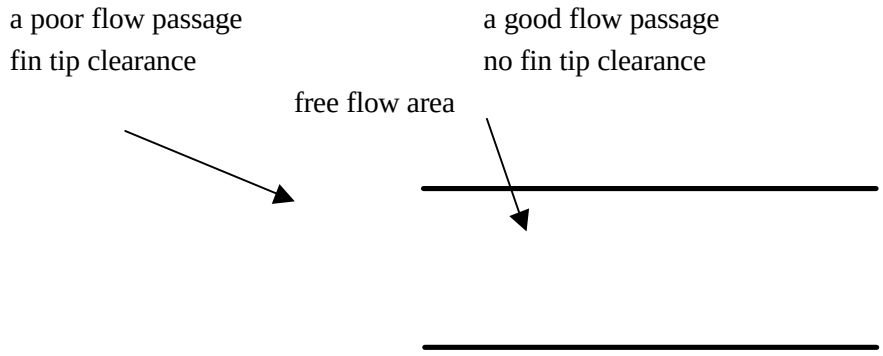


**Figure 4.5.3: Recommendation for finned surface flow passages, in which the free flow area is created by adjusting the fin pitch, i.e., the spacing between parallel fins. The opposing surface 'touches' the fin tips.**

Figure 4.5.4 shows the experimental results for the type II flow passage. This passage differs from the type I passage in that the fins are staggered. Figure 4.5.4 shows that this flow passage behaves as a cylindrical duct with equal hydraulic diameter. This conclusion also holds for the non-staggered passage. Also shown is that the staggered arrangement is much less sensitive to enlarging the free flow area by providing clearance between opposing fins. The explanation for this behaviour might be that, due to the staggering, a larger scale for the lateral turbulence is created which distributes the mass flow more evenly across the full free flow area.

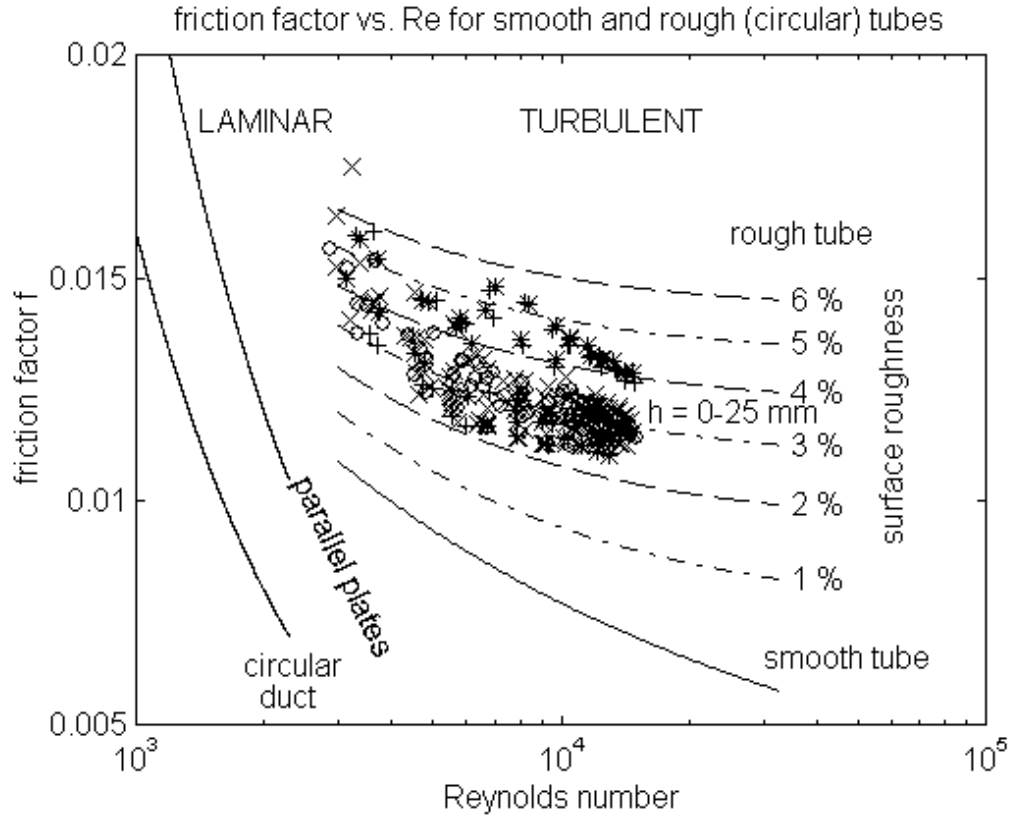


**Figure 4.5.4: Experimental results type II staggered fins.**

Figure 4.5.5 shows the comparison of the friction-factor/Reynolds-number correlation for the staggered and the non-staggered fin arrangement. The staggered arrangement results in a higher friction factor only for the range of low Reynolds numbers which is representative for the flue gas flow. For those applications where a higher pressure drop on the flue gas side can be tolerated, staggered fins may be better than non-staggered fins.

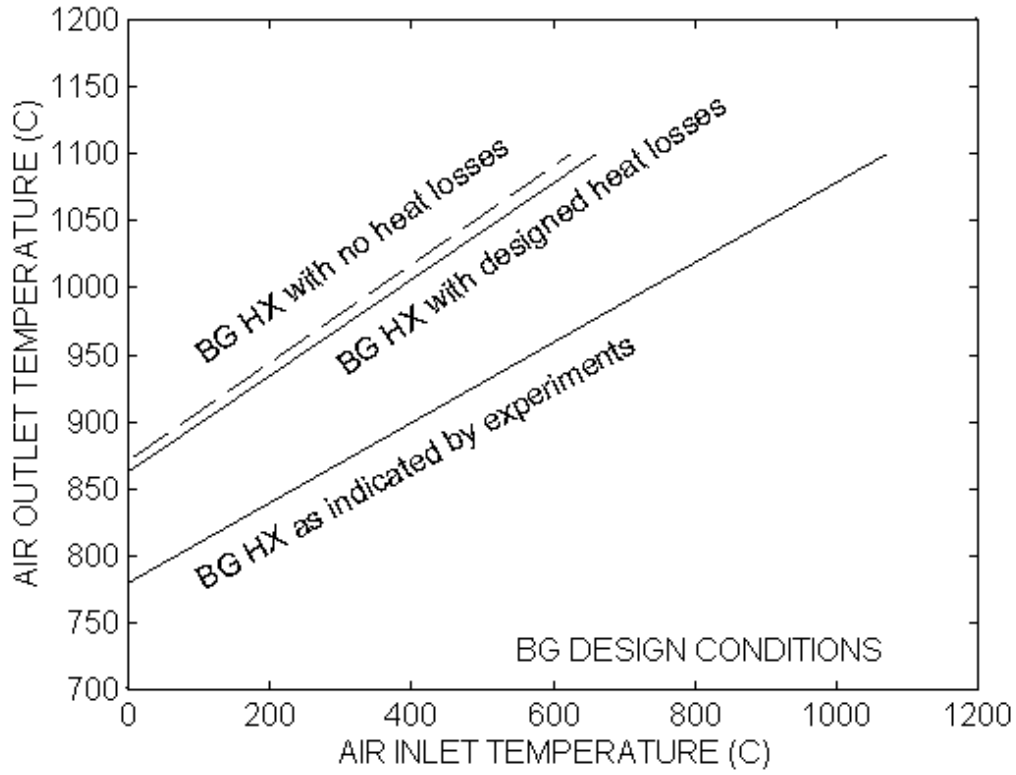


**Figure 4.5.5: Comparison staggered / non-staggered fin arrangement.**

#### 4.5.2.5 Summary of the Main Results

These experimental findings show that the length of the fins should be as high as possible to provide the maximum heat exchange area. Fin tip clearance should be avoided in thick fin flue gas recuperators. The free flow area that needs to be provided in order to match the pressure drops should be incorporated in between adjacent fins. If heat exchangers are to be designed with a standard set of finned elements, the designer should work such that the hydraulic diameter of the flow passages is not larger than the fin tip clearance.

### 4.5.3. Analyses of the CECON Heat Exchangers

This section describes the results of a numerical simulation of the pressure drop and heat exchange in the CECON heat exchanger that has been tested at BG Technology (see chapter 4.6).

#### 4.5.3.1 Description of the CECON Heat Exchanger at BG Technology

Table 4.5.3 list the full geometry of the CECON Heat Exchanger in terms of the relevant heat exchanger parameters. The heat exchanger is built by stacking 20 SCHUNK CaRSIC-NT elements on top of each other. A solid tube is inserted inside of the elements to provide a free flow area of 79.5 $cm^2$ for the combustion flue gases The outer tube that encases the elements provides a free flow area of 52.2 $cm^2$ for the combustion air stream.

The fin efficiency reference heat transfer coefficients are also listed in Table 4.5.3. Due to the very high thermal conductivity of silicon carbide and due to the short height of the fins, the reference heat transfer coefficient for a fin efficiency of 95 % measures 48 $W/m^2 \cdot K$ for the flue gases and 68 $W/m^2 \cdot K$ for the combustion air. The actual heat transfer coefficients that are reached within the heat exchanger are of the order of 30 $W/m^2 \cdot K$. Thus the fin efficiencies of the CECON heat exchanger are very high and conductive resistances of the fins can be neglected.

Table 4.5.3 lists also the heat exchanger areas. For the flue gases, the heat exchange area consists of the finned element internal area, 663.7 $cm^2$, and the surface area of the internal solid tube, 89.0 $cm^2$. The hydraulic diameter is 19 mm. The internal solid tube is very important in the heat exchange equation because it distributes the heat evenly. For the combustion air, the heat exchange area consists of the finned element external area, 729.5 $cm^2$, and the internal surface of the encasing tube, 257 $cm^2$. The resulting hydraulic diameter is 9.58 mm. The radiative heat transfer between the finned elements and the internal solid tube and external outer casing should definitely not be neglected.

The fin tip clearance on the combustion product side measures 20 mm. This is of the order of the hydraulic diameter. On the air side, the fin tip clearance measures 4 mm which is much smaller than the hydraulic diameter. It should not expected that the free flow area that is created by the fin tip clearances negatively affects the flow distribution and, thus, the fin exchange capacities.

| SCHUNK CarSIC-NT FIN INTERNAL | | |
|---|---|---|
| fin base length excl. base roundings | 35.0 | mm |
| fin overall height include. Roundings | 15.0 | mm |
| fin (mean) foot print chord | 11.0 | mm |
| fin (mean) wet perimeter | 36.0 | mm |
| fin (max) cross section | 58.7 | $mm^2$ |
| fin wetted skin area | 1377.1 | $mm^2$ |
| fin foot print area | 386.1 | $mm^2$ |
| fin efficiency ref. heat transfer coef h95 | 48.0 | $W/m^2 \cdot K$ |
| fin efficiency ref. heat transfer coef h90 | 102.5 | $W/m^2 \cdot K$ |
| **SCHUNK CarSIC-NT TUBE INTERNAL** | | |
| element bare area | 0.00270 | $m^2$ |
| element fin area | 0.066104 | $m^2$ |
| free flow area (minimal, with no fin clearance or $\phi$=103 mm) | 0.00274 | $m^2$ |
| flow length | 0.04500 | m |
| hydraulic diameter (minimal) | 0.00610 | m |
| hydraulic diameter (with solid tube used) | 0.01820 | m |
| **SCHUNK CarSIC-NT FIN EXTERNAL** | | |
| fin base length excl. base roundings | 35.0 | mm |
| fin overall height include. Roundings | 15.0 | mm |
| fin (mean) foot print chord | 12.2 | mm |
| fin (mean) wet perimeter | 38.2 | mm |
| fin (max) cross section | 89.2 | $mm^2$ |
| fin wetted skin area | 1517.9 | $mm^2$ |
| fin foot print area | 425.2 | $mm^2$ |
| fin efficiency ref. heat transfer coef h95 | 67.6 | $W/m^2 \cdot K$ |
| fin efficiency ref. heat transfer coef h90 | 144.3 | $W/m^2 \cdot K$ |
| **SCHUNK CarSIC-NT TUBE EXTERNAL** | | |
| element bare area | 0.00009 | $m^2$ |
| element fin area | 0.07286 | $m^2$ |
| free flow area (minimal, with no fin clearance or $\phi$=175 mm) | 0.00326 | $m^2$ |
| flow length | 0.04500 | m |
| hydraulic diameter (minimal) | 0.00804 | m |

**Table 4.5.3: Relevant CECON heat exchanger characteristics**

#### 4.5.3.2 Heat Exchanger Model

The model of the heat exchanger has been outlined in previous deliverables. The model solves the energy balances for the finned tube elements and takes into account convective heat exchange with the gas

streams; radiative hat transfer between the element surfaces, and axial conduction along the inner solid insert, the finned elements and the external outer casing. The model assumes that the surfaces behave as black bodies with respect to thermal radiation because silicon carbide has a very high emissivity, and because the free space between the fins act as black body cavities. From numerical experiments, it can be concluded that the axial conduction in the heat exchanger is negligible in comparison with the convective heat exchange; and that the heat radiation on the flue gas side of the exchanger between the inside surface area of the finned elements and the solid inserts are negligible as well. The radiative energy transfer between the external surface of the finned elements and the outer casing is not negligible. This radiative transfer of energy to the external casing is in turn transferred by convection to the air stream.

The convective heat transfer is modelled using the Colburn-Reynolds analogy. The ratio of the Colburn-j factor to the friction factor f is set to 0.35. This is a normal value for these kinds of heat exchanger flow passages. The advantage of this approach is that the ratio between pressure drop and heat exchange is guaranteed to correspond with the reality.

#### 4.5.3.3 Numerical versus Experimental Results

Table 4.5.4 lists the results of selected experiments at BG Technology. Table 4.5.5 shows the results of matching the numerical results from the simulation program with the experimental results from the testing at BG Technology. The input data for each simulation were the flue gas inlet temperature and the air stream outlet temperature. This table lists the computed required air inlet temperature, the computed flue gas outlet temperature, the computed heat exchanges, and the computed friction factor *f* in order to match the air side pressure drop and the heat exchange.

| **Parameter** | **Units** | **1** | **4** | **6** | **8** | **10** |
|---|---|---|---|---|---|---|
| *Flue Gas* | | | | | | |
| Flow Rate | kg/hr | 114.9 | 142.4 | 176.0 | 174.3 | 184.3 |
| Inlet temperature | °C | 631 | 985 | 879 | 1211 | 1356 |
| Outlet temperature | °C | 324 | 534 | 517 | 697 | 771 |
| Pressure drop | Pa | 34 | 116 | 88 | 114 | 125 |
| *Air Stream* | | | | | | |
| Flow Rate | kg/hr | 121.1 | 120.8 | 121.5 | 120.5 | 120.2 |
| Inlet temperature | °C | 28 | 32 | 23 | 30 | 33 |
| Outlet temperature | °C | 342 | 580 | 499 | 757 | 888 |
| Pressure drop | Pa | 101 | 127 | 112 | 233 | 175 |

**Table 4.5.4: BG Technology CECON Heat Exchanger Test Results**

| Parameter | Units | 1 | 4 | 6 | 8 | 10 |
|---|---|---|---|---|---|---|
| *Flue Gas* | | | | | | |
| Flow Rate | kg/hr | 114.9 | 142.4 | 176.0 | 174.3 | 184.3 |
| Inlet temperature | °C | 631 | 985 | 879 | 1211 | 1356 |
| Outlet temperature | °C | 323 | 540 | 518 | 702 | 780 |
| Pressure drop | Pa | 92 | 306 | 267 | 357 | 465 |
| *Air Stream* | | | | | | |
| Flow Rate | kg/hr | 121.1 | 120.8 | 121.5 | 120.5 | 120.2 |
| Inlet temperature | °C | 23 | 28 | 23 | 35 | 24 |
| Outlet temperature | °C | 342 | 580 | 499 | 757 | 888 |
| Pressure drop | Pa | 252 | 114 | 296 | 408 | 480 |
| *Heat exchange* | | | | | | |
| Q desorbed from gas | kW | 12.0 | 23.5 | 22.7 | 33.2 | 40.3 |
| Q absorbed by air | kW | 11.1 | 19.5 | 16.9 | 26.0 | 31.4 |
| Q loss | kW | 1.0 | 4.3 | 6.1 | 7.8 | 9.8 |
| Q gain - radiation | kW | 0.1 | 0.6 | 0.4 | 0.6 | 0.9 |
| *f* friction factor | | 0.024 | 0.024 | 0.022 | 0.0245 | 0.027 |

**Table 4.5.5: Simulation results to match the experimental data**

The surprising results from the experiments were the extremely low pressure drops. The main reasons why the actual performance of the heat exchanger differs from the design are:

1. For the design of the heat exchanger, a conservative estimate of the pressure drop due to the contraction/expansion in between the elements was taken into account. Following the results of the experimental pressure drop program, it must now be recognised that these pressure drops are surprisingly almost negligible. Indeed, the thick fins behave as continuous fins with no interruption. This is a major conclusion from this program.

2. The pressure drops for the experiments at BG Technology are too low to be matched with the simulation. Without violating the Colburn analogy, these pressure drops cannot be matched.

3. The surprisingly high value of the friction factor. The experimental data suggest a value for the friction factor as high as 0.025. This value is derived from the analysis of the gas-to-air heat exchange (Colburn analogy). Such a high value can be found in compact heat exchangers with offset fins, but is unlikely for the flow passages that are encountered in the CECON heat exchanger.

4. The surprisingly high values of the heat losses of the exchanger. The design was based upon a heat loss of 10% of the nominal heat exchange capacity. The actual performance of the heat exchanger suggest a relative heat loss as high as 25%. On a total exchange capacity of about 40 kW, these heat losses are very important. In the heat exchanger model, the heat losses are modelled as convective cooling of the outer casing. The performance data of the heat exchanger suggest that the

heat losses may be due to conductive losses at the heat exchanger headers. These end losses are hard to predict if the actual conductive heat path and thermal boundaries are not known. They are not included in the model.

Figure 4.5.6 shows the computed air outlet temperature as a function of the computed air inlet temperature for the BG heat exchanger as built and for the BG heat exchanger as designed. For a medium degree of air preheat, the difference between the two cases is negligible. However, for a high degree of combustion air preheat, the difference is substantial.

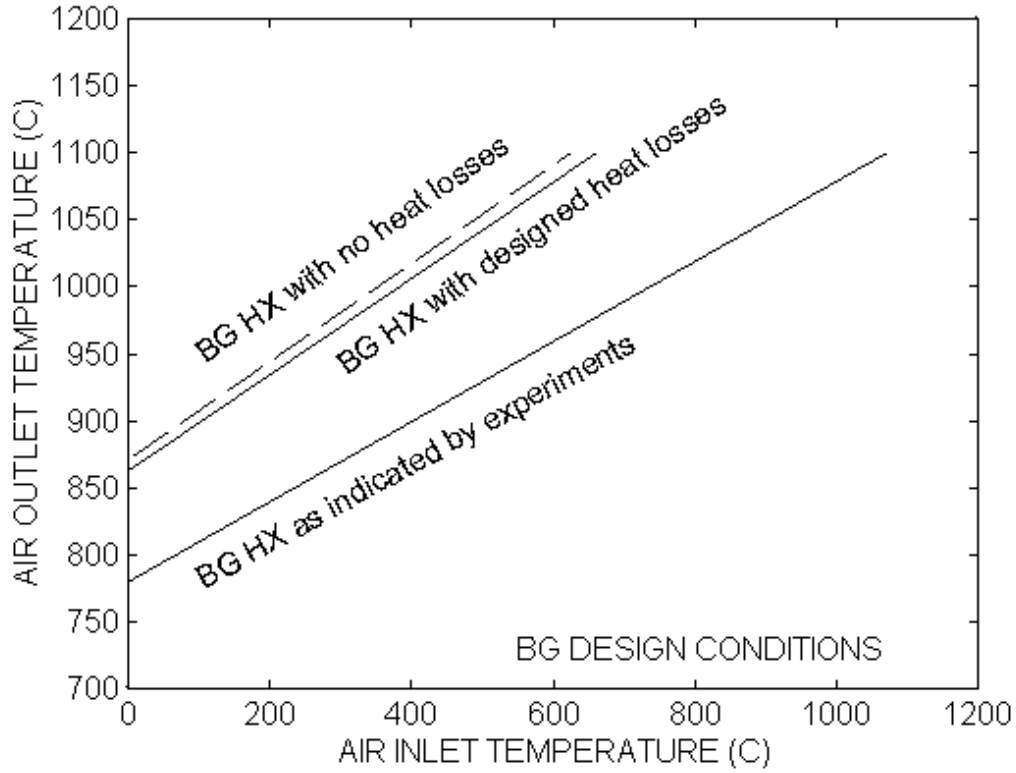


**Figure 4.5.6: Effect of heat losses of the heat exchanger on the exchanger preheat capacity.**

#### 4.5.3.4 Summary of the Results Achieved

There are conflicting results between the simulation model and the experimental results. The friction factor that is suggested by the experiments is too high. At this moment, further research and experiments are needed to clarify this issue. In particular, cold flow experiments on experimental tubes with a length at least 100 times the hydraulic diameter should be performed.

The relative high heat loss of the experimental rig, even though that the heat exchanger was indeed insulated with great care, should serve as warning to future designers. At the high temperatures that are encountered in these applications, apparently very small heat leakage paths can deteriorate the performance of the heat exchanger substantially.

## 4.6 Task 5, Development of the Ceramic Heat Exchanger

(Contractor: BG plc., Great Britain , assisting party: Gaz de France, France)

### 4.6.1 Introduction

The overall objective of Task 5 is to design, construct and experimentally test a compact ceramic counterflow gas to gas heat exchanger, which is to be used to raise the thermal efficiency of fossil fuelled industrial processes. The heat exchanger should be capable of operating in process environments up to 1400°C and achieve energy savings of up to 60%. The heat exchangers will exploit the thermal and mechanical properties of monolithic ceramic materials to maximise the cost-effectiveness for installation on new processes and for retrofitting to existing processes. These are to be based on a modular design concept and engineering designs, which could be used for a range of heat exchangers from 60kW to 500kW thermal capacity, will be produced. A sample design heat exchanger will be experimentally tested as part of Task 5 to validate its thermal performance. Other sample heat exchangers will be produced for preheating combustion air with both the premix radiant surface burner from Task 2 (see chapter 4.3) and the non-premix radiant surface burner from Task 3 (see chapter 4.4).

A methodology for calculating and optimising the heat transfer and pressure loss characteristics of the heat exchanger is being developed by the Katholieke Universiteit Leuven (KUL) and is described in chapter 4.5 (Task 4). Results from the BG plc heat exchanger will be correlated against the predictions from KUL, and will be used to set key model parameters and validate the model. This model can then be used to arrive at optimised engineering designs for the basic ceramic module and a range of heat exchanger designs for use in processes with thermal input from 60kW to 500kW.

### 4.6.2 Materials Selection for Compact High Temperature Heat Exchangers (Task 5A)

#### 4.6.2.1 Introduction

In order to achieve the overall objectives of Task 5, it was essential that the most appropriate monolithic ceramic was chosen for the key components of the heat exchanger. The aims of Task 5A were to select the appropriate material, based on commercial and published data, and determine its limits of operation using a range of thermomechanical property tests, including flexural strength, oxidation, thermal shock and thermal cycling.

After discussions with materials suppliers, it was decided that the optimum ceramic would be an isostatically pressed and green machined grade of reaction bonded silicon carbide (RBSC) supplied by Schunk Ingenieurkeramik GmbH. Schunk were also in the process of developing finned heat exchanger elements based on this material.

#### 4.6.2.2 Materials

The RBSC material, CarSIK-NT®, was supplied in slab form by Schunk Ingenieurkeramik GmbH. Test bars, of dimensions (65x4x3)mm were machined from the slabs and their edges chamfered. The test bars were lapped on all four sides using 14↘m diamond paste.

#### 4.6.2.3 Experimental

The experimental programme was carried out jointly between BG plc and Gaz de France ref [15] and included a comparison and standardisation of mechanical testing procedures. The objective of the experimental programme was to determine the effective operating thresholds for RBSC in high temperature environments simulative of heat exchanger operation. The high temperature test methodology comprised flexural strength testing (up to 1400°C), oxidation in air and simulated combustion products (SCP), thermal shock and thermal cycling. The methodology was developed by *British Gas plc ref [15],* Gaz de France and Penn State University (ref [16 and 17]).

#### 4.6.2.4 Results & Discussion

##### 4.6.2.4.1 Mechanical Strength

The materials testing and evaluation programme demonstrated that CarSIK-NT® RBSC had sufficient stability at high temperatures (up to 1350°C) providing it was not subjected to severe thermal cycles. Its high temperature strength properties were typical of other RBSCs and siliconised SiC material. Below 1300°C, a small increase in strength was observed due to oxidative healing of surface flaws on exposure to such temperature. At 1400°C and above, the free silicon began to soften and this was reflected in the greatly reduced strength.

##### 4.6.2.4.2 Oxidation

***Oxidation in Air***

In the case of oxidation for 200 hours, temperatures above 1000°C were required to create a uniform oxide scale. The higher the temperature, the more protective the oxide layer. The amorphous silica formed was initially composed of nodules ("seeds") which coalesced and fused as the temperature rose and, finally, at 1400°C, formed a continuous layer of vitreous silica. In addition, all of the specimens contained a second phase; crystallised aluminosilicate. It took the form of crystallised compounds at the lower temperatures and of a second layer above the silica at 1300°C and 1400°C, which may have resulted from a dissolution reaction of the crystallised nodules by the vitreous silica.

Oxidation penetrated into the ceramic at 1300°C and above, combined with silicon exudation at the highest oxidation temperature (1400°C). Silicon oxides and pores displaced the silicon from its channels underneath the surface of material. For this reason, 1400°C was considered too high for long term applications.

***Oxidation in SCP***

The material displayed largely passive oxidation behaviour, with very thin, uniform oxide layers produced below 1300°C. The increased oxidation rate and high mobility of silicon above 1400°C produced a different type of oxide growth. At these temperatures, the silicon exuded from the material and formed distinct globules in and on the oxide layer. This effect was thought to contribute to the near surface porosity found in specimen cross-sections. Bearing in mind these observations along with the strength data, there was concern over the long term stability of this material to oxidising environments above 1400°C. Below this temperature there was sufficient passivity to preserve the material's integrity, particularly in light-loading conditions.

***Comparison of Oxidation in SCP and Air***

On the basis of the present results, the SCP atmosphere reduced the rate of mass gain at high temperature, compared to oxidation in air. Furthermore, it showed higher retained strengths below the ultimate temperature for long-term application (1400°C). The occurrence of silicon exudation was not affected by the oxidation atmosphere, however, evidence of internal oxidation in SCP was not apparent up to 1400°C, compared to 1300°C in air.

The present results appear to conflict with previous studies of RBSC oxidation. In general, steam containing environments promote the devitrification of the oxide layer, which in turn promotes increased oxidation. Although there was little difference in the mass gains below 1300°C, at 1400°C the mass gain in air was substantially higher than in SCP. It is feasible that these differences may have resulted from the slightly different experimental set-ups used for the oxidation tests (e.g. different gas flow rates and alumina or SiC specimen supports). The test facilities are known to influence oxidation behaviour (ref [18]).

#### 4.6.2.4.3 Thermal Shock

There are no concerns over the material's ability to withstand thermal shock. The material was resistant to rapid water quenching up to 400°C, but underwent a severe reduction in retained strength above this temperature. Whilst this technique was not necessarily representative of heat exchanger operating conditions, it demonstrated that the material has sufficient robustness to resist the mild thermal shocks which could occur during operation of the heat exchanger.

#### 4.6.2.4.4 Thermal Cycling

The resistance of this material to such mild thermal shock was amply illustrated by its performance in series A thermal cycling tests. The thermal cycling tests represented the likely consequences of significant transient variations of combustion product or pre-heated air temperatures. The material had excellent resistance to thermal cycles between room temperature and intermediate temperatures (<1100°C, series A). It should be borne in mind, however, that the 5 minutes hold time did not allow sufficient cooling time to actually reach ambient air temperature. Such cycles resulted in mild oxidation, alone.

Series B, which cycles between intermediate and higher temperatures (up to 1400°C) resulted in extensive damage to the material. The damage was manifest as deformation, porosity, silicon exudation,

external/internal oxidation and fracture of SiC grains. This damage was particularly severe after the 1100°C<->1400°C cycle, but much less acute after the 1000°C<->1300°C cycle. After this latter cycle, it was considered that the material retained sufficient integrity and strength to satisfy any concerns over its performance.

Similarly to the material's oxidation behaviour, its thermal cycling properties were thought to be related to the mobility of the free silicon present in the material. Exposure to high temperatures allowed the silicon to exude from the surface and accelerate the oxidation process. Cooling to intermediate temperatures produced a contraction of the material, which resulted in increased internal stresses and the fracturing of the SiC grains in areas of high residual density.

Evidence for this mechanism was provided by the series of tests using the 1050°C<->1350°C thermal cycle. It was clear that damage could occur after just a few cycles, however, in the early stages, this was manifest only as silicon exudation. As the number of cycles increased, the silicon was further displaced from the porous areas and, eventually, this resulted in extensive disruption and damage to the SiC microstructure.

### 4.6.3 Joining and Fabrication of Heat Exchanger (Task 5B)

#### 4.6.3.1 Introduction

The objectives of Task 5B were to evaluate the optimum method(s) for the joining and fabrication of heat exchanger elements. The proposed heat exchanger design included a modular assembly of several (up to 20) finned, cylindrical elements. It was essential, firstly, that this assembly had sufficient robustness during fabrication of the heat exchanger unit and, secondly, that this structural integrity was maintained and able to provide gas tightness during operation.

Two basic joining techniques, self-bonding and high temperature ceramic adhesive, were selected.

#### 4.6.3.2 Joining Techniques

##### 4.6.3.2.1 Self Bonding

It was proposed that a combination of capillary flow by molten or softened silicon, combined with a brief period of passive oxidation, could provide an adequate bond between relatively smooth RBSC component surfaces. This technique required short exposures to high temperature, oxidising environments.

An initial study examined the bonds formed in RBSC plate material at temperatures of 1350°C, 1400°C and 1430°C, using a variety of interface conditions. Subsequent joints were attempted at temperatures of 1300°C, 1350°C and 1400°C, using sectioned heat exchanger segments and dwell times between 2 hours and 40 hour. No pressure was applied to the joints during bonding.

##### 4.6.3.2.2 High Temperature Ceramic Adhesives

Trial samples of a number of high temperature ceramic adhesives were supplied by PI-KEM Ltd (6 Greenhill Rod, Camberley, Surrey, GU15 1PE, UK). Ceramabond® 503 and Ceramabond® 668 were selected due to their applicability to silicon carbide based ceramics, along with another three adhesives, Ultra-Temp® 516, Ceramabond® 569 and Ceramabond® 618.

The RBSC specimens, including those machined from the heat exchanger segments did not represent the ideal joint design. Firstly, the mating surfaces were both flat and relatively smooth. Secondly, it was not possible to make allowances in the design for thermal expansion mismatch and mechanical stress. Thus, maximum bond strengths could not be expected. In practice, however, the bonds were only required in the first instance to provide sufficient stability to enable manufacture of the heat exchanger. The main function during service was to provide gas tightness, with provision for structural integrity a secondary factor.

Joints were fabricated from machined heat exchanger segments using, where practical, the recommended application and curing procedure for each of the five ceramic adhesives.

#### 4.6.3.3 Results

##### 4.6.3.3.1 Self Bonding

Although many of the successful bonds had adequate handling strength, several broke during sectioning (using a diamond slitting wheel), mounting and polishing. The most detailed evaluation was carried out on the specimens from the preliminary joining trials.

At 1400°C, smooth (machined) mating surfaces produced a very good joint with a thin (~6µm) uniform layer of silicon metal at the bond interface. The RBSC adjacent to one side of the bond contained significant porosity, however. There was also evidence of oxidation near the edge of the bond. Rough (as cast) mating surfaces at 1400°C also produced good bonds, however, the silicon metal which filled the interface was much less uniform and contained a significant proportion of oxide. In addition, the RBSC on both sides of the bond contained small levels of porosity. The addition of silicon grit at the interface of 1400°C bonds resulted in a partially silicon filled joint interface. The interface between the silicon and RBSC consisted of a thin layer of oxide, and there was also porosity in one of the RBSC sections adjacent to the bond.

At 1430°C, smooth mating surfaces produced a much thicker layer of silicon at the bond interface, although this contained significant voidage. Oxide was also prevalent at the silicon-RBSC interface and there was no porosity in the RBSC adjacent to the bond. A rough mating surface at 1430°C also produced a very good bond, although the significantly increased bond space was completely filled with silicon (at an average thickness of 40mm). This silicon layer was almost completely encapsulated by oxide and the near surface RBSC was extremely porous on one side of the bond. The addition of silicon grit at the interface of 1430°C bonds was more successful than at 1400°C and resulted in the almost complete filling of the bond interface with silicon. An uneven oxide layer was apparent at the silicon-RBSC interface, although there was no porosity in the RBSC.

After the main joining trials, successful bonds were only formed at 1400°C and the longest dwell time (40 hours) at 1350°C. The 20 hours at 1400°C and 40 hours at 1400°C bonds were oxidised for 200 hours in air at 1300°C and 1350°C, respectively. These exposures produced small, identical weight gains. The bond oxidised at 1300°C was examined after sectioning and polishing. The bond was filled with a mixture of silicon and oxide, and there was no porosity in the adjacent RBSC. There was some discontinuity in the bond near regions which contained a significantly greater proportion of oxide.

#### 4.6.3.3.2 High Temperature Ceramic Adhesives

All of the high temperature ceramic adhesives produced successful bonds, which had sufficient strength for light handling. Manual fracturing of the bonds demonstrated that, although the adhesives were the weak link, there was good bonding between the adhesive and RBSC, and a much high bond strength than self bonding. In terms of ease of application and resulting bond appearance, 503 produced the best results.

Air oxidation tests were carried out on ceramic adhesive joined specimens, for 200 hours at 1300°C and 1350°C. All of the specimens underwent small weight gains and there were slight differences in the manifestation of oxidation between the specimens. There was a distinct glazing of the RBSC adjacent to the 516, 569 and 618 adhesively bonded specimens, which is not normally found on RBSC materials oxidised at 1300°C. The oxidised joints had retained handling strength, although all of the bonds, apart from 503 and 618, fractured during sample preparation. Optical microscopy of cross-sections through 503 and 618 bonds were only partially successful, as it appeared that much of the bond material was lost during sample preparation.

### 4.6.3.4 Discussion

The experimental work demonstrated that successful bonds can be formed between RBSC specimens using either high temperature ceramic adhesives or self bonding. The main advantage of self bonding was that it required no additional material or interlayers. Furthermore, bonds could be formed over a period of time simply from exposure to temperatures above 1350°C. Despite these obvious advantages, the technique would have serious drawbacks if applied to the RBSC heat exchanger. Firstly, the heat exchanger segments would have to be pre-joined prior to assembly of the heat exchanger unit (involving the provision for a large, high temperature furnace). Secondly, there would be no guarantee that the complete heat exchanger assembly would be exposed to temperatures above those required for the formation of self bonded joints. Parts of the unit may always be at much lower temperatures and, as such, may not be able to form bonds.

It was clear that a suitable high temperature ceramic adhesive would provide the best alternative to a self bonded structure. Although, in the present work, the bonds were formed under non-ideal conditions, all of the test joints had adequate strength for handling and much higher strengths than self bonded joints. This was particularly important, as it was entirely feasible to manufacture heat exchanger segment modules (of, for example, 6 or 7 segments) prior to installation in the furnace. The adhesives have also confirmed their inherent resistance to high temperatures and suffered no degradation during oxidation tests.

It was thus proposed that a high temperature ceramic adhesive be used to prefabricate heat exchanger segment modules prior to installation in the furnace. This was the recommended method for the manufacture of the trial heat exchanger units at both BG plc and Gaz de France. After installation the adhesives would benefit from being under compression during service and there would be a very low risk of failure of the bonds. On balance, the most appropriate adhesive for this function was Ceramabond® 503.

### 4.6.4 Heat Exchanger Design and Fabrication (Task 5C)

#### 4.6.4.1 Initial Design Concept

The heat exchanger selected for the CECON project is a counterflow system utilising ceramic elements supplied by Schunk Ingenierkeramik GmbH (figure 4.6.1). This is the RBSC material capable of withstanding the temperatures required ref [19].
For the purposes of the CECON Project, inlet and outlet flow parameters and temperatures were specified. These are shown in the schematic, figure 4.6.2.

In order to achieve the required temperatures utilising the existing furnace at the BG Technology Gas Research & Technology Centre (GRTC), it was initially proposed that the furnace would need to be operated at 100kW instead of 50kW at achieve combustion product temperatures of ~1400°C. Based on the design of the Schunk elements, an estimate was produced by KUL (ref [20]) for the initial design arrangement of the heat exchanger, for 100kW. However, in order to achieve the required preheat temperature of 1100°C, the heat exchanger height was prohibitively high for the furnace used for the experiments. Therefore, an alternative arrangement was sought to allow the heat exchanger to be operated over the required range, whilst using a heat exchanger with a height that could be accommodated on the furnace at the GRTC. A method was proposed for preheating the air prior to entering the heat exchanger.

#### 4.6.4.2 Heat Exchanger Design

The design itself comprised a vertical stack of 20 Schunk elements. In order to channel the flow, an inner and outer tube were obtained, based on design calculations provided by KUL. The top and bottom "header" sections of the heat exchanger were designed so that they did not provide an excessive pressure drop, and could be used to effectively compress the heat exchanger elements, figure 4.6.3.

The design of the heat exchanger carefully ensured that the refractory and ceramic components were kept in compression, keeping tensile forces to a minimum. This was particularly important at the hotter (lower) end of the heat exchanger.

Former figure 5.1

**Figure 4.6.1: Illustration of the Schunk element**

**Former figure 5.2**

**Figure 4.6.2: Schematic of the CECON-unit**

### 4.6.4.3 Design of Gaz de France (GdF) Heat Exchanger

As part of the CECON Project, the ceramic heat exchanger comprising the Schunk elements was to be integrated with the radiant burners developed as part of Tasks 2 and 3.

KUL were asked to supply dimensions and number of elements for the GdF heat exchanger. The excess air was the same as for the BG Technology heat exchanger, but the net thermal input was set at 50kW, instead of the 100kW used at BG Technology. The temperature conditions of 1400°C combustion product temperature and 1100°C preheat were still used, with the same restrictions on maximum pressure drop across the heat exchanger. KUL supplied these figures based on their current simulation.

The heat exchanger supplied to GdF was constructed with the inner tube external diameter, and outer tube internal diameter specified from these simulations.

former figure 5.3

**Figure 4.6.3: Final assembly**

.

### 4.6.5 Experimental Testing (Task 5D) (ref [22])

#### 4.6.5.1 Experimental Arrangement

The general schematic arrangement for the furnace and heat exchanger used at BG Technology during the testing is shown in figure 4.6.4a.

This illustrates the furnace with the heat exchanger located at the flue outlet. A separate air preheater is shown to heat up the "cold" air introduced into the heat exchanger. The hot air from the heat exchanger is discharged along with the combustion product gases (CPG) into the laboratory extract system.

**Figure 4.6.4a: Schematic of the heat exchanger, furnace and preheater arrangement**

### 4.6.5.2 Instrumentation

In order to assess the performance of the heat exchanger, a range of measurements were employed to determine the volume flow and mass flow rates of the air and combustion product gases as well as their temperature. In addition, pressure drop data was obtained in order to determine the friction factor for this type of heat exchanger. As indicated earlier, provision was made at the design stage for the various types of instrumentation used.

The measurements taken from the heat exchanger are schematically shown in figure 4.6.4b, and described in more detail below.

**Figure 4.6.4b: Schematic of the instrumentation arrangement**

- The furnace temperature was measured using an unshielded R-type thermocouple inserted through the roof of the furnace and data from this was manually recorded. The combustion product gas temperature at the inlet and outlet to the heat exchanger was measured using R-type ceramic shielded thermocouples with the air inlet and outlet temperatures being measured using ceramic shielded K-type thermocouples. All of these measurements were recorded on a datalogger, so that a visual graphical display could be used to assess whether the heat exchanger was at or near to thermal equilibrium condition.

- Pressure drop measurements across the heat exchanger were performed using liquid manometers. Two pressure tapping locations were used to determine the pressure drop on the air side of the heat exchanger, whilst only one point was used for the combustion product side. The reason for this was that the combustion products were exhausted to atmosphere, so it was reasonable to use this as the negative pressure side for the pressure drop determination. All the pressure measurements were manually recorded.

- The flows to the burner and heat exchanger used on the test furnace were taken from the available rotameters and a turbine meter. These figures for the actual volume flow rates were manually recorded, and subsequently corrected to Metric Standard Conditions (MSC - 1013mbar, 15°C).

- The composition of the combustion gases was made at the inlet to the heat exchanger. The excess air of the burner was determined from the oxygen concentration, and also CO was measured to ensure that complete combustion had occurred, and that there was no combustion within the heat exchanger. In addition to the measurements at this point, oxygen measurements were made at the combustion product outlet from the heat exchanger, in order to determine the air leakage into the combustion product gas stream, and a measurement of carbon dioxide at the air outlet to determine if there was any combustion product leakage into the air stream.

#### 4.6.5.3 Test Scheme & Technical Issues

The initial test programme plan comprised cold air testing followed by tests at increasing temperatures, up to the full proposed 1400°C combustion product gas temperature and 1100°C air temperature from the heat exchanger. However, a number of technical problems prior to and during the testing phase resulted in changes to this programme and timescales.

- During the initial re-commissioning of the furnace and testing, problems were encountered with the electronic ratio control device failing or causing the burner to lockout. This device was eventually removed from the burner logic, as it was not required for the tests on the heat exchanger.

- Initial tests using preheated air as the "cold" air through the heat exchanger, with no combustion, highlighted some temperature control problems with the preheater. This preheater, although readily available, had originally been sized for a burner in excess of 450kW and this resulted in no effective temperature control. Modification to the preheater allowed good temperature control by preventing a number of elements from operating, however further difficulties were encountered at preheats in excess of 200°C. The preheater needed to be operated with flow rates lower than those for which it was originally designed and this, coupled with the operational mode of individual heating elements either being fully on or off, could result in individual elements overheating, due to the reduced convective heat transfer. Indeed, with increasing preheat air temperatures, problems were encountered with overheating elements and smoking. It was therefore not possible to operate with preheated air in excess of 200°C.

- During the very highest temperature tests (combustion product gas temperature ~1400°C), a local hot spot was observed on the bottom casing of the heat exchanger. This resulted in tests at the highest temperatures being curtailed to avoid serious damage to the heat exchanger structure. However, it was still possible to operate the heat exchanger over a reasonable range of temperatures to obtain validation data.

#### 4.6.5.4 Tests & Results

##### 4.6.5.4.1 Cold Air Tests

Initial cold air tests were conducted on the heat exchanger to obtain some data on pressure drop, in order to allow KUL to make some initial calculations of friction factor, and assess whether the pressure drop figures were reasonable compared to the predictions. These experiments were only performed on the air side of the heat exchanger, as it was not possible to perform these tests on the combustion product side. This was due to limitations in being able to measure representative cold volume flow rates equivalent to the volume flows for combustion products at 1400°C.

##### 4.6.5.4.2 Hot Tests

A number of hot tests were performed on the heat exchanger up to combustion product temperatures approaching 1400°C. It was found during the tests that it was not possible to achieve the required temperatures using the 100kW (net) burner rating originally proposed, and this was eventually set at 140kW, with 10% excess air.

***Rig Operation***

The experiments were performed by initially lighting the furnace at a low thermal input, with the water loads fully inserted, in order to minimise thermal shock to any of the ceramic or refractory components (including the shielded thermocouples). The thermal input was increased to the 140kW (net) and the air flow trimmed to deliver 10% excess air, as determined by the flue gas oxygen. Further increases in furnace temperature were achieved by slow retraction of the water loads from the furnace, until these were flush with the furnace inside wall. Around 3-4 hours were required, from burner light-up, to reach an equilibrium condition. The cold air flow rate to the heat exchanger was set to be equivalent to the combustion air requirement at 140kW and 10% excess air.

***Tests With Preheat***

In addition to the tests with cold air, preheated air was also introduced into the heat exchanger. Tests were only conducted with a preheated air set point of 200°C due to problems with the preheater as described above.

***"Cooling" Tests***

Tests were conducted at a fixed thermal input and excess air, with varying furnace temperatures. The furnace temperature was slowly reduced from the highest temperatures by slowly introducing the cooling loads back into the furnace. Following this, it was possible to observe the temperatures falling until an equilibrium was reached.

#### 4.6.5.4.3 Material Performance

Two elements were placed inside the furnace prior to the tests. This allowed a quick assessment to be made of the effects of the high combustion product temperatures on the ceramic elements following the experimental test programme.

### 4.6.5.5 Discussion

#### 4.6.5.5.1 Pressure Drop Characteristics

For combustion product gases at 1382°C the differential pressure was 146Pa. This is significantly lower than the upper design limit of 500Pa. Similarly, under these conditions, the differential pressure for the air was 470Pa, again lower than the limit of 2000Pa, although in this case, the air exit temperature was 771°C, somewhat lower than the 1100°C that would produce the high pressure drops.

#### 4.6.5.5.2 Heat Exchanger Performance

Examining the "cooling" tests data shows that with a combustion product temperature of 1306°C, air temperatures of 776°C were achieved. During other tests where equilibrium may not have been fully reached, with combustion product temperatures of 1382°C and 189°C air preheat being used, an exit air temperature of 859°C was achieved.

In order to quantify the performance of the heat exchanger, an effectiveness has been determined (ref [23]). This determination produces figures for the effectiveness of the heat exchanger of between 66% and 73%, figure 4.6.5

Former figure 5.5.

**Figure 4.6.5: Heat exchanger effectiveness**

This was determined by using the following equation:

$$Effectiveness = \frac{C_{hot}(T_{CPGin} - T_{CPGout})}{C_m(T_{CPGin} - T_{AIRin})}$$

where, $C_m = C_{cold}$ = mass flowrate (air) x $C_p$ (air in),
$C_{hot}$ = mass flowrate (CPG) x $C_p$ (CPG in),
$T_{CPGin}$ is the temperature of the CPG in to the heat exchanger,
$T_{CPGout}$ is the temperature of the CPG out of the heat exchanger,
and, $T_{AIRin}$ is the temperature of the air in to the heat exchanger.

The higher figures are recorded for the highest combustion product gas temperatures.

#### 4.6.5.5.3 Assessment of Leakage

In the design phase of the heat exchanger (ref [24]), there was concern regarding the possible leakage of air into the combustion product stream, or combustion products into the air stream. During the experimental tests, measurements were taken to assess the amount of leakage which might be occurring.

The measurements of the concentration of oxygen in the combustion product gases entering the heat exchanger, compared to the combustion products exiting the heat exchanger, indicated that there was between 1 and 1.5%, by volume, of air leaking from the air side of the heat exchanger.

An assessment of whether any combustion product gases were leaking into the air stream was also made. It was expected that due to the greater pressures associated with the air side of the heat exchanger, that no combustion product leakage would occur, however, measurements of the carbon dioxide concentration in the air outlet stream did detect some $CO_2$. From these measurements, it was assessed that the leakage in this direction was no more than 0.85% by volume. The reason for this leakage is peculiar to the method used to test this heat exchanger, where it is possible for the absolute pressure of the combustion products entering the heat exchanger to be higher than the absolute pressure of the air exiting the heat exchanger. Normally, this air stream would be introduced to the burner, and would be at a significantly higher absolute pressure.

#### 4.6.5.5.4 Evaluation of Material Performance

***Elements Placed Inside the Furnace***

The visual examination of the two reaction bonded silicon carbide (RBSC) elements placed inside the furnace confirmed that these elements had been exposed to temperatures in excess of the recommended heat exchanger material limit of 1350°C.

The RBSC suffered extensive silicon exudation, which was mainly located on the surfaces of the inner fins and at the base of both the inner and outer flow channels. The material was also covered by a relatively thick oxide glaze. The presence of such a thick oxide glaze, combined with the silicon exudation provides ample evidence that the material was exposed to temperatures above 1400°C. It also suggests that the material was subjected to significant temperature fluctuations.

The examination of the two RBSC elements reaffirms the conclusions reported previously (ref [19]), which state that the material is suitable for long term operation at temperatures of 1300-1350°C depending on the extent of thermal cycling. Operation of the heat exchanger at higher temperatures clearly may result in blockage of the flow channels and, hence have adverse effects on its performance.

***Heat Exchanger Elements and the Heat Exchanger Itself***

At the end of the testing, the heat exchanger was dismantled to examine the various components. The refractory in the bottom section had some small cracks, with a significant crack also visible in the central tube support. The SiC central tube was removed intact, although this had changed colour, possibly due to the iron content in the tube, and changes in its oxidation state. This appeared to have caused a discolouration to the inner fins of the Schunk elements, particularly at the lower, hotter end of the heat exchanger. Significantly, there was no visible damage to the elements, and no silicon exudation.

The bonds between the elements were intact, although these could broken with less physical force than before the heat exchanger had been used. However, there was no visible sign of any gaps between the elements which would have been responsible for any leakage. In the lower parts of the heat exchanger there was no evidence of self bonding.

### 4.6.6 Main results Achieved

CarSIK-NT® reaction bonded silicon carbide has excellent strength retention up to 1350°C, above which the strength falls due to softening of free silicon.

The material has good stability for long-term exposure to oxidising environments at temperatures up to 1300°C

The material is damaged by extensive transgranular cracking after water-quench thermal shocks from temperatures of 400°C and above.

The material is also susceptible to microstructural damage after extensive thermal cycling with peak temperatures of 1300°C and above. The damage is extremely severe with a peak temperature of 1400°C, leading to deformation, loss of free silicon, external/internal oxidation and fracture of SiC grains.

The material shows good resistance to the intended duty. The material operating limits defined in this work have been incorporated into the heat exchanger design studies (Task 5C), and validated in the experimental testing (Task 5D).

Self bonding can be used to join RBSC specimens at temperature above 1350°C; the method relies on capillary action of silicon, which fills the void between the mating surfaces.

High temperature ceramic adhesives produce stronger joints between RBSC specimens and have good resistance to high temperature oxidation.

A counterflow heat exchanger utilising the reaction bonded silicon carbide elements supplied by Schunk Ingenierkeramik GmbH, has been designed, fabricated and assembled.
The heat exchanger to be used at GdF in conjunction with radiant burners, has also been designed, fabricated and assembled at GdF.
The counterflow heat exchanger has been tested and has been successfully operated up to temperature ~1400°C, however operational problems prevented extended testing at these temperatures. In addition, problems with the design of the available preheater did not allow tests to achieve 1100°C outlet air temperatures.

The pressure drops measured for this design of heat exchanger are low.

An effectiveness of ~70% has been determined for this design of heat exchanger.

Although leakage between combustion gas stream and air stream has not been completely eliminated, this has been determined to be no more than ~1.5% for air leakage into the combustion product stream, and less than 1% of combustion product gas leakage into the air stream.

Assessment of the RBSC materials placed in the furnace support the performance measurements made in the earlier material tests.
The bonding technique used for the experimental heat exchanger remained intact during the testing programme.

## 4.7 Task 6, Validation of the Burners with Internal Recuperation

(Contractor: Gaz de France, France)

### 4.7.1 Introduction

The prime objective of the CECON Project is the development of a radiant surface burner with internal recuperation, that has high efficiencies and low emissions. This clean and efficient energy conversion process is a combination of two units: a radiant surface burner and a ceramic heat exchanger (see figure 4.6.2). Two types of premixed radiant burner has been developed by ACOTECH within this project (Task 2, see chapter 4.3), the first one based on a perforated fibre (FeCr Alloy) mat, the other on a nit fibre (same Alloy) mat. The ceramic heat exchanger has been designed by BG plc (Task 5, see chapter 4.6). Consequently, two versions of the « CECON Unit » have been built and tested by GAZ DE FRANCE that is reported hereafter.

Each « CECON Unit » has a capacity of around 50kW (in term of gas input) and is composed of the heat exchanger which preheats the combustion air using the energy of the combustion products, and of one of the radiant surface burners enclosed in an enclosed casing to ensure the internal recuperation of the combustion products.

This chapter details the design of the « CECON Units » and its construction. It presents the test bench on which they have been characterised, then the tests performed and finally the results.
The overall objective of Task 6 is the validation of the compatibility of the use of preheated combustion air with the concept of radiant surface burners as well as the validation of the energy saving potential of the integrated process i.e. the validation of a new high efficiency and low pollutant emissions heating equipment.
The two premixed radiant surface burners have been first characterised on GDF's test equipment in terms of :

- The operating range in the radiant mode: the gas and air flow rates, pressure, gas temperature and net caloric value of the gas were measured. The air factor was determined by analysis of the premixture.

- Combustion product analysis: was carried out for a reference air factor at three different gas inputs. The $O_2$, $CO_2$, $CH_4$ and $NO_X$ concentrations were measured also for an intermediate output

and the maximum output at three air-gas ratios. Flue gases were collected just below the radiant panel.

- Emissivity and temperature: in the same conditions as above, directional spectral emissivity and temperature were measured by pyrolaser at the centre of the panel.

- Radiation efficiency: was determined for one panel direction (horizontal panel radiating vertically downwards). The results give the radiation efficiency of the surface as a function of gas input (fixed air factor) and as a function of air factor (fixed gas input).

The same characterisation tests as above have been carried out on both « CECON Units ». Thus comparisons were made between the burners in an open atmosphere and the burners mounted in a sealed casing equipped with a quartz glass and coupled with an air/flue gases collecting exchanger.
In addition, tests were performed on the enclosed perforated burner with cold air (i.e. without the heat exchanger).

Under the framework of the "CECON" Project, GAZ DE FRANCE used its specific test bench for radiant burners including all associated measurement devices.

### 4.7.2 Design of the « CECON Unit » and Description of the Four Tested Equipment

#### 4.7.2.1 Description of the ACOTECH Radiant Surface Burners

One burner supplied by ACOTECH was coated with a knitted metallic fibre mat and the other with perforated metallic fibre mat. The walls of both burners were made of heat-resistant materials. A complete description of these burners is provided in chapter 4.3 and in ref [25]. The burners were supplied through an external mixer with the air-gas mixing.

#### 4.7.2.2 Description of the Heat Exchanger

A complete description of the heat exchanger designed is given in chapter 4.6 and in ref [24].

#### 4.7.2.3 Design of the « CECON Units »

To collect the combustion products just below the radiant surface burners it was necessary to design a specific device. In this way an enclosed casing was the chosen solution (see figure 4.7.1). It was made of stainless steel. The inside of the chamber was isolated using a rigid heat-resistant material.

The heat exchanger was coupled with the outlet of the enclosed casing of the burner. The collected hot air was then sent to the external mixer through stainless steel pipes.

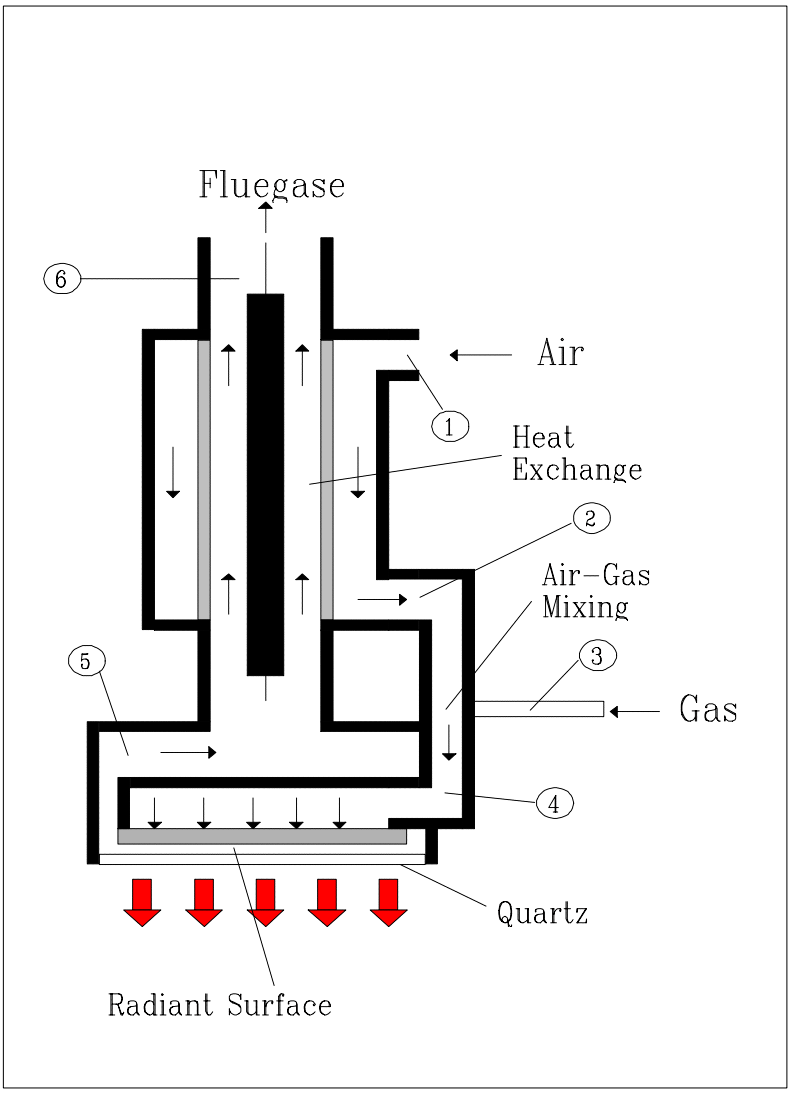


| points | 1 | 2 | 3 | 4 | 5 | 6 |
|---|---|---|---|---|---|---|
| measurements | temperature | temperature | temperature, NCV of the natural gas | temperature, mixing analysis | temperature fluegas analysis | temperature fluegas analysis |

**Figure 4.7.1: Final assembly of the « CECON unit »**

Besides the assembly of the heat exchanger (problems of alignment of the internal pieces as already discussed in ref [24]), the major encountered difficulty in the construction of the « CECON Unit » was due to the large dimensions and heavy weight of the ceramic heat exchanger. Some modifications of GAZ DE FRANCE's test bench were necessary to withstand the heat exchanger.

#### 4.7.3.4 The Four Tested Equipment

| Number | Description | Designation |
|---|---|---|
| Burner 1 | Nit metal fibre mat ACOTECH burner in open air | Non-enclosed nit burner |
| Burner 2 | Perforated fibre mat ACOTECH burner in open air | Non-enclosed perforated burner |
| Burner 3 | CECON Unit composed by the nit metal fibre mat ACOTECH burner and the BG heat exchanger | Enclosed nit burner |
| Burner 4 | CECON Unit composed by the perforated metal fibre mat ACOTECH burner and the BG heat exchanger | Enclosed perforated burner |

**Table 4.7.1: The four tested combinations burners and combustion air from the open air/preheated in the heat exchanger**

### 4.7.3 Test Methods

#### 4.7.3.1 Description of the Test Bench

The radiant efficiency is the ratio of the radiant flux emitted by a radiation source toward the half space formed by the source's plane to the power consumed by the source. To measure the radiant energy emitted, GAZ DE FRANCE has a specific test bench made up a vertical 90° arc of a circle equipped with six thermopiles located every 20°. It can thus describe a quarter sphere of a radius of 2.385 m, whose centre is coincidental with that of the emitting surface (see figure 4.7.2).

This quarter sphere is divided into n small surfaces Si around each thermopiles. The measured values (i.e. the irradiance Ei which is the quantity of energy received per unit area and per unit of time measured by each thermopile) are corrected to take into account radiation absorption due to such factors as the presence of water vapour in the atmosphere. Then the radiating power P is calculated by the formula :

$$P = \frac{\sum_{i=1}^{n} Si \,.\, Ei}{1 - e}$$

and the radiant efficiency is :

$$h = \frac{P}{I}$$

where ε is the emissivity corresponding to the absorption of the water vapour in the air (ε # 0.03), and I the gas input.

**Figure 4.7.2: Radiant efficiency measurement, horizontal panel radiating vertically downwards**

#### 4.7.3.2 Measured Parameters and Measurement Method

The measured parameter was the irradiance from the burner received by each thermopile located on the measurement arc in order to determine the radiant efficiency.

The flow rate of gas and air was measured using volume-meters. The air-gas mixing supplied to the burner was also analysed to find the air-gas ratio (n).

The temperatures of the air, air-gas mixing and flue gases were measured on the exchanger, using thermocouples (see figure 4.7.1 the measurement points). Combustion products were analysed at the inlet and at the outlet of the exchanger in order to determine the CO, $CO_2$, $O_2$ and $NO_X$ concentrations.

For the non-enclosed burners the surface temperatures of the metallic fibre mats were measured using a "PYROLASER" optical pyrometer with a narrow spectrum range centred on the 0.865 mm wavelength (0.865 mm ± 0.015). Such measurements are valid for temperatures between 600 and 1500°C. It was used for measurements between 2 and 10 m, and at distances of 0.2, 0.4, 0.8 m. The pyrometer was also used to measure the emissivity of the metallic fibre mats.

Tests were done as soon as the assembly (burner, casing and exchanger) temperature was stabilised: due to the inertia of the heat exchanger, a day was needed between each gas input setting change to stabilise the temperature.

### 4.7.4 Tests and Results

#### 4.7.4.1 Tests Performed

Tests were performed in February and March 1998 using the four heating equipment in a downward vertical emission position (see figures 4.7.3 and 4.7.4).

##### 4.7.4.1.1 Non-enclosed Burners

The following measurements were taken on both burners:

- Radiant efficiency for power densities of 100/250/400 kW (NCV)/m², i.e. gas inputs of 12.5/31.25/50 kW (NCV) with an air-gas ratio (n) of 1.05, and also for a power density of 250 kW/m² with air-gas ratios of 1.15/1.30/1.50.
- Surface temperatures of the metallic fibre mats.
- Combustion product analysis near the radiating surface.

##### 4.7.4.1.2. Enclosed Burners

The following measurements were taken on the both enclosed burners:

- Radiant efficiency for power densities of 100/250/350 kW (NCV)/m², i.e. gas inputs of 12.5/31.25/43.75 kW (NCV) with an air-gas ratio (n) of 1.05, and also for a power density of 250 kW/m² with air-gas ratios of 1.15 and 1.30.
- Temperatures of the air and flue gases at the exchanger's inlet and outlet, and the air-gas mixing at the burner's inlet.
- Combustion product analysis at the exchanger's inlet and outlet.

Due to a significant air leakage in the exchanger and because of the limited air flow rate in the installation, the tests at 400 kW(NCV)/m² were replaced with tests at 350 kW(NCV)/m², and the test with a air-gas ratio of 1.50 was not performed.

##### 4.7.4.1.3 Enclosed Perforated Burner with Cold Combustion Air

The following measurements were taken in cold air, using the burner with a perforated metallic fibre mat:

- Radiant efficiency of the quartz glass at a power density of 250 kW(NCV)/m².

**3: Picture of GDF test bench with the « CECON unit »**

**Figure 4.7.4: Picture of the « CECON unit » in operation**

#### 4.7.4.2 Results

##### 4.7.4.2.1 Non-enclosed Burners

The radiant efficiency is shown in function of the power density and of the air-gas ratio in figures 4.7.5 and 4.7.6. The analyses of the combustion products are shown in table 4.7.2.
The radiant efficiency for the burners were similar, i.e. 44% for a power density of 250 kW(NCV)/m².

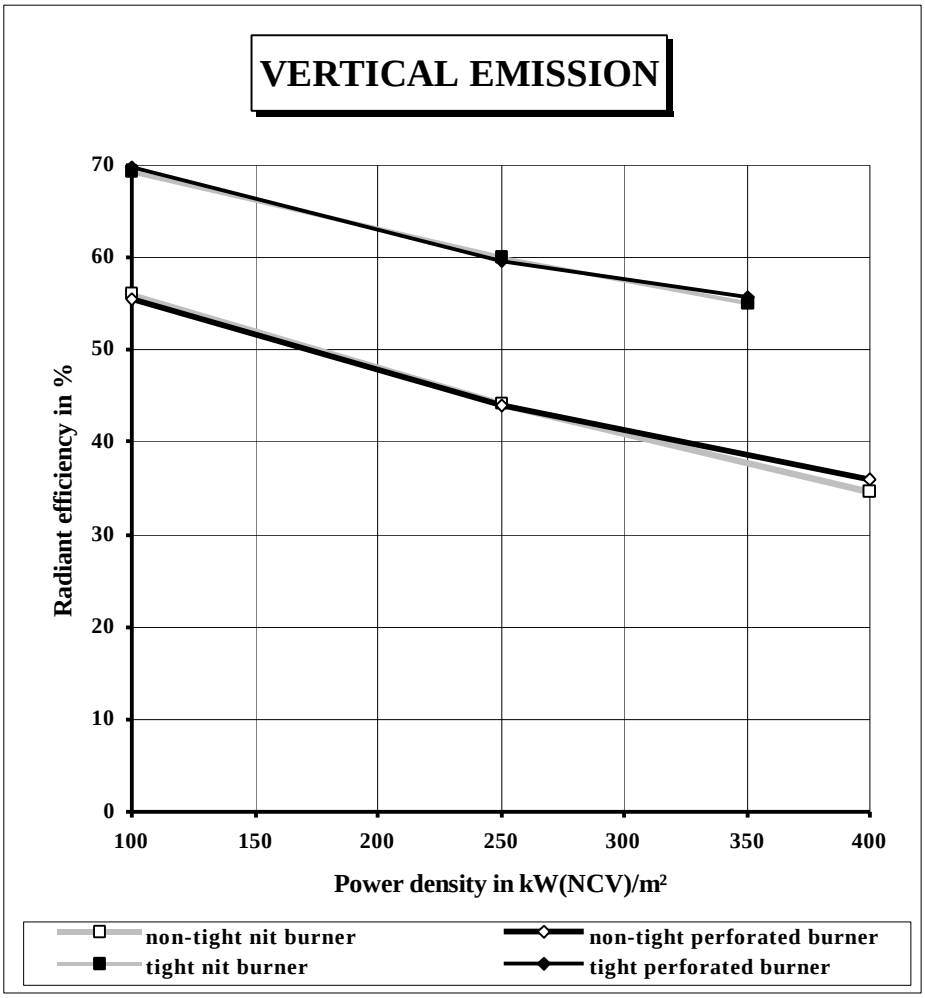


| Power density kW(NCV)/m² | 100 | 250 | 350 | 400 |
|---|---|---|---|---|
| Non-enclosed nit burner | 56.1 | 44.2 | - | 34.6 |
| Non-enclosed perforated burner | 55.5 | 44.0 | - | 35.9 |
| Enclosed nit burner | 69.3 | 60.0 | 55.0 | - |
| Enclosed perforated burner | 69.8 | 59.5 | 55.7 | - |

**Figure 4.7.5 : Radiant efficiency function of the power density at an air-gas ratio of 1.05**
**Comparison between non-enclosed burners and enclosed burners**

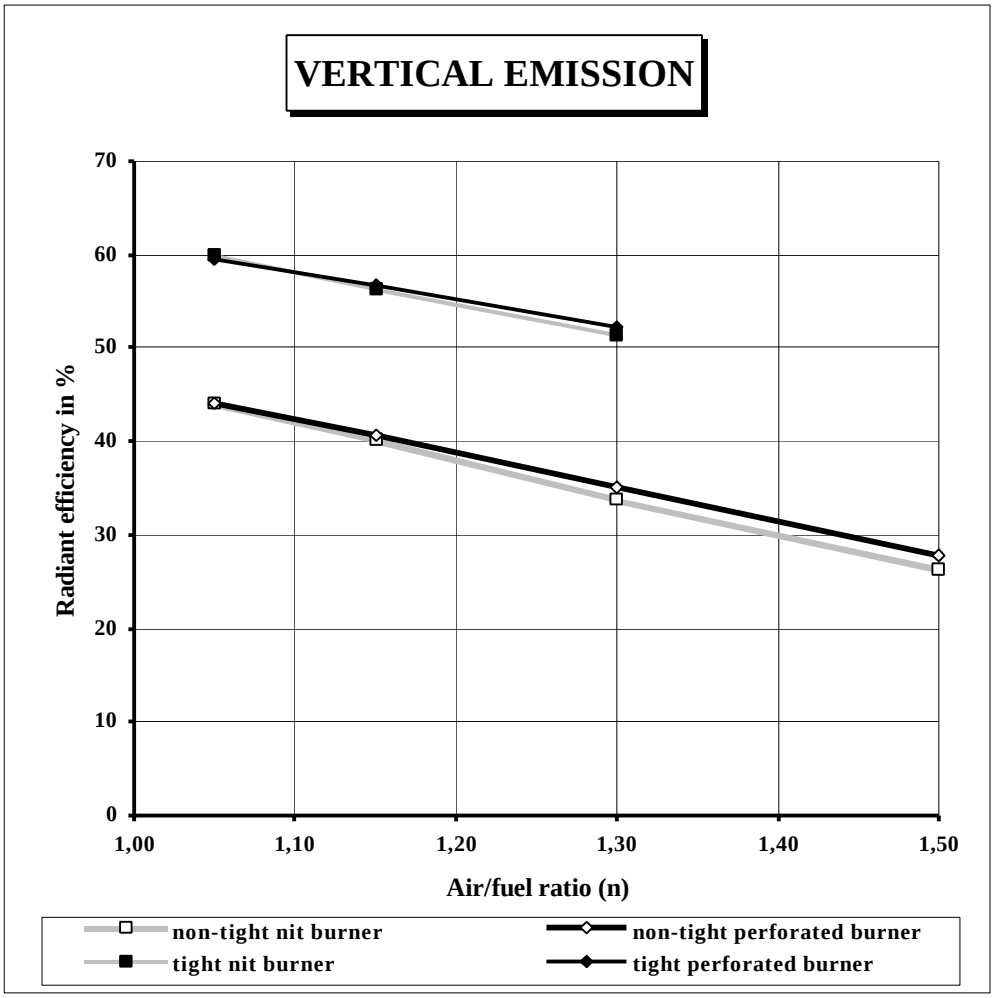


| Air-gas ratio | 1.05 | 1.15 | 1.30 | 1.50 |
|---|---|---|---|---|
| Non-enclosed nit burner | 44.2 | 40.2 | 33.9 | 26.4 |
| Non-enclosed perforated burner | 44.0 | 40.7 | 35.1 | 27.8 |
| Enclosed nit burner | 60.0 | 56.4 | 51.3 | - |
| Enclosed perforated burner | 59.5 | 56.7 | 52.3 | - |

**Figure 4.7.6 : Radiant efficiency function of the air-gas ratio at a power density of 250kW(NCV)/m$^2$ Comparison between non-enclosed burners and enclosed burners**

## *Nit burner*

| POWER DENSITY kW/m² | Air/fuel ratio n | $NO_X$ ppm | $O_2$ % | CO % | $CO_2$ % | $CO/CO_2$ | Pressure of the Mixing mbar |
|---|---|---|---|---|---|---|---|
| 100 | 1.05 | 6 | 9.04 | 0.0130 | 7.16 | 0.0018 | 0.15 |
| 250 | 1.05 | 22 | 1.1 | 0.0470 | 11.28 | 0.0042 | 0.60 |
| 400 | 1.05 | 34 | 1.08 | 0.0530 | 11.28 | 0.0047 | 1.10 |

## *Perforated burner*

| POWER DENSITY kW/m² | Air/fuel ratio n | $NO_X$ ppm | $O_2$ % | CO % | $CO_2$ % | $CO/CO_2$ | Pressure of the Mixing mbar |
|---|---|---|---|---|---|---|---|
| 100 | 1.05 | 5 | 10.1 | 0.0140 | 6.0 | 0.0023 | 0.11 |
| 250 | 1.05 | 19 | 1.5 | 0.0400 | 11.1 | 0.0036 | 0.40 |
| 400 | 1.05 | 37 | 1.04 | 0.0300 | 11.4 | 0.0026 | 0.85 |

The flue gas analyses aren't precised because of the natural dilution of the combustion products.

**Table 4.7.2 : Flue gas analyses for the two non-enclosed burners**

#### 4.7.4.2.2 Enclosed Burners Coupled with the Heat Exchanger

The radiant efficiency is shown in function of the power density and of the air-gas ratio in figures 4.7.5 and 4.7.6.

The test results are given in tables 4.7.3 and 4.7.4.

Due to a significant air leakage in its lower part, the exchanger could only provide hot air between 170 and 200°C. The extent of this leak was determined as part of the test at 100kW/m². For a proper supply to the burner, the amount of air at the exchanger's inlet had to be three times larger. The combustion products analysis confirmed the significance of the leak. Thus the tests could not be performed properly due to this large leak which was not possible to remove.

It has to be noted that there are very large differences between tables 4.7.3 and 4.7.4 for the combustion products analysis. For the tests of table 4.7.3, the flue gases were regularly sampled at the exchanger's inlet, using a tube. For the tests of table 4.7.4, they were sampled by suction using the tube installed on the exchanger. In both cases the $NO_x$-emissions are rather low with less than 10ppm at 3% $O_2$.

The radiant efficiency was very similar for both enclosed burners with a supply of hot air, i.e. 15 points above the efficiency of non-enclosed burners. For a power density of 250 kW(NCV)/m², the radiant efficiency was approximately 60%. However, these results should be considered in their context. As a matter of fact, the glass surface was twice as large as the burner's radiating surface. Part of the radiation went through the quartz glass. But the quartz glass had a large radiation output because it was very hot. That's why test with cold combustion air were also performed.

| **Power density** | **100 kW/m²** | **250 kW/m²** | | | **350 kW/m²** |
|---|---|---|---|---|---|
| **Air/fuel ratio (n)** | **1.05** | **1.05** | **1.15** | **1.30** | **1.05** |
| ***Temperature in °C*** | | | | | |
| **Air entry exchanger** | 23 | 24 | 23 | 24 | 25 |
| **Air exit exchanger** | 161 | 189 | 190 | 179 | 177 |
| **Air/Gas mixing** | 148 | 194 | 195 | 189 | 195 |
| **Fluegases entry exchanger** | 483 | 696 | 707 | 720 | 802 |
| **Fluegases exit exchanger** | 57 | 77 | 78 | 77 | 83 |
| ***Pressure in mbar*** | | | | | |
| **Air entry exchanger** | 6.0 | 40.2 | | | 84.5 |
| **Air exit exchanger** | 4.6 | 17.4 | | | 26.2 |
| ***Fluegas analyses entry exchanger*** | | | | | |
| **CO** | 0.015 | <0.005 | | | <0.005 |
| **$CO_2$** | 10.5 | 2.0 | | | 0.2 |
| **$O_2$** | 2.6 | 17.2 | | | 20.8 |
| **$NO_X$** | 6.5 | 4.8 | | | 0.3 |
| ***Fluegas analyses exit exchanger*** | | | | | |
| **CO** | 0.012 | <0.005 | | | <0.005 |
| **$CO_2$** | 9.3 | 6.1 | | | 5.0 |
| **$O_2$** | 4.6 | 10.1 | | | 11.9 |
| **$NO_X$** | 6.0 | 13.6 | | | 22.0 |

**Table 4.7.3: Flue gas analyses and temperatures for the enclosed NIT burner**

| Power density | 100 kW/m² | 250 kW/m² | | 350 kW/m² |
|---|---|---|---|---|
| **Air/fuel ratio (n)** | **1.05** | **1.05** | **1.15** | **1.30** | **1.05** |
| ***Temperature in °C*** | | | | | |
| **Air entry exchanger** | 23 | 27 | 25 | 26 | 25 |
| **Air exit exchanger** | 183 | 204 | 200 | 191 | 189 |
| **Air/Gas mixing** | 158 | 197 | 195 | 190 | 193 |
| **Fluegases entry exchanger** | 467 | 698 | 708 | 725 | 819 |
| **Fluegases exit exchanger** | 72 | 84 | 85 | 86 | 93 |
| ***Pressure in mbar*** | | | | | |
| **Air entry exchanger** | 6.4 | 41.5 | | | 88.5 |
| **Air exit exchanger** | 3.8 | 13.0 | | | 28.7 |
| ***Fluegas analyses entry exchanger*** | | | | | |
| **CO** | 0.008 | <0.005 | | | <0.005 |
| **$CO_2$** | 10.56 | 7.50 | | | 5.38 |
| **$O_2$** | 2.42 | 7.70 | | | 11.24 |
| **$NO_X$** | 6.6 | 18.0 | | | 29.0 |
| ***Fluegas analyses exit exchanger*** | | | | | |
| **CO** | 0.007 | <0.005 | | | <0.005 |
| **$CO_2$** | 7.94 | 5.46 | | | 2.68 |
| **$O_2$** | 6.86 | 11.30 | | | 16.20 |
| **$NO_X$** | 6.0 | 14.0 | | | 14.5 |

**Table 4.7.4: Flue gas analyses and temperatures for the enclosed perforated burner**

#### 4.7.4.2.3 Enclosed Perforated Burner with Cold Combustion Air

The results are given in table 4.7.5.

For the test at 250 kW(NCV)/m², the radiant efficiency measured with cold air was approximately 6 points lower than the efficiency measured with air at 200°C, i.e. 53.7% instead of 59.5%. These results proved the clear interest of the recuperation of the combustion products energy to preheat the combustion air in order to increase the radiant efficiency.

### 4.7.5 Summary of the Main Results Achieved

In the framework of Task 6 of the CECON project, GAZ DE FRANCE has designed, built and tested two « CECON Units » i.e. combinations of a premixed radiant surface burner and a ceramic heat exchanger in a view to preheat the combustion air by the combustion products and thus to increase the radiant efficiency of these heating equipment. The radiant surface burners have been

| | hot air | cold air |
|---|---|---|
| ***Radiant efficiency in %*** | | |
| | 59.5 | 53.7 |
| ***Temperatures in °C*** | | |
| **Air/gas mixing** | 197 | 38 |
| **Fluegases** | 698 | 692 |

**Table 4.7.5 : Comparison of the results obtained for the enclosed perforated burner with hot and cold air at a power density of 250(NCV)/m$^2$**

Developed in the framework of the contract by ACOTECH (Task 2) and the ceramic heat exchanger by BG plc (Task 5).Some difficulties have been encountered: air leakage in the heat exchanger which was not possible to remove. Due to it, the combustion air temperature was limited to around 200°C. Nevertheless it was observed that the radiant efficiency of a «CECON Unit » with a combustion air at 200°C is 60%, around 15 points higher than those of the premixed burner alone (i.e. an increase of ca 35%), as it was foreseen. With higher preheated air it could have been possible to increase even more the efficiency.

The size and weight of the heat exchanger is not compatible with a direct industrial application of an enclosed radiant surface burner. Some additional works are needed to design a more compact system and easier to manufacture.

## 5. CONCLUSIONS

*Task 1, Safety Design for Premix Surface Burners*

1a In order to predict the resulting pressure peak height in the event of the ignition of the gas-air mixture within a closed premix burner, a design rule has been postulated and verified which depends upon the ratio of the volume of the air/gas mixture that is ignited to the total burner-system volume (burner + cover + heat exchanger).

1b A safety device consisting of a ceramic foam which fills up the volume in the burner unit, by its porous structure, lets the gas-air mixture pass through with only a small pressure drop has been tested satisfactory.

1c The design rule has been validated by comparison of the results of explosion tests with the safety device and the results without the safety device. The explosion tests showed that this device acts satisfactory and that the design rule is valid up to temperatures of the gas/air mixture of 500 °C.

*Task 2, Development of the Premix Surface Burner*

2 The premix radiant surface gas burners using burner surfaces made of sintered and knitted metal fibre mats performed well, and showed no ageing or degradation after endurance tests corresponding to 2 years operation under the design conditions.

*Task 3, Development of the Non-Premix Surface Burner*

3 The non-premix gas burner designed had a serious problem inherent to the design. This was due to excessive heating of the fuel gas by the combustion air before the fuel gas entered the mixing/combustion chamber, the fuel gas cracked and formed soot that destroyed the prototypes.
An alternative design of non-premix radiant burner in which the fuel was not heated has been established. The concept operated satisfactory without preheating of the combustion air, although $NO_X$-emissions were high. However, when the combustion air was preheated to 400°C, the burner broke down.

*Task 4, Modelling of the Ceramic Heat Exchanger*

4a Experiments showed that the fact that the fins with rough surface and rounded tips in the flow passage of a heat exchanger were not continuous strips of solid material did not affect the friction-factor/Reynolds-number correlation. Furthermore it was shown that about 20 to 25 % of the installed heat exchanger surface can be 'lost' due to flow channelling when the fin tips are separated. The offset fin arrangement yields a 10 to 15 % higher friction factor for the range of Reynolds number of 2000 to 4000.

4b The construction of an actual industrial heat exchanger should be done with great care. The experience that was gathered from the project indicate that, at high temperatures which are encountered in the applications envisioned, spurious heat leakage paths may seriously deteriorate the performance of the heat exchanger.

*Task 5, Development of the Ceramic Heat Exchanger*

5a CarSIK-NT (trade name) reaction bonded silicon carbide used in the heat exchanger showed excellent performance for heat exchanger material up to 1300°C.

5b It has been proven that the heat exchanger designed, constructed and tested under well defined operational conditions is able to transfer 70% of the thermal energy available in the flue gas to the combustion air. Further to this, the heat exchanger showed a relatively low-pressure drop.

*Task 6, Validation of the Burners with Internal Recuperation*

6a The radiant efficiency (the ratio of the radiant flux emitted by a radiation source to the power consumed by the source) of both the premix radiant gas burners is 44% for a power density of 250 kW(NCV)/$m^2$. In order to gather the combustion gases an enclosure containing a quartz window was developed. The use of this enclosure increased the radiant efficiency to 54% (power density of 250 kW(NCV)/$m^2$).
After connecting the burners and the casing to the ceramic heat exchanger, the radiant efficiency increased to 60% at a power density of 250 kW(NCV)/$m^2$ and with preheated air of 200°C.

6b The $NO_X$-emissions of the premix radiant burners coupled with the heat exchanger (« CECON Unit ») were rather low, at less than 10 ppm at 3% $O_2$. The emissions of CO were negligible.

*General conclusion*

7 Although this project demonstrates the principle of the « CECON Unit », the size and weight of the heat exchanger is not compatible with a direct industrial application of a enclosed radiant surface burner. Some additional works are needed to design a more compact system and which is easier to manufacture.

## 6. EXPLOITATION PLANS

In the following table the exploitation intentions of the results obtained in the project have been summed.

| **Title of the exploitable result** | **Parties (result owners) involved** | **Exploitation intention** |
|---|---|---|
| Safety Design Premixed Radiant Burners | N.V. Nederlandse Gasunie | - Dissemination to third parties<br>- Consultancy |
| Sintered Metal Fibre Burner Mat out of Coarser Fibre. | N.V. Acotech S.A. | None, for commercial reasons |
| High-end Knitted Metal Fibre Burner Mat | N.V. Acotech S.A. | Exploited by Acotech for Industrial Radiant Infrared Applications |
| Design of the Housing of a Premix Radiant Metal Fibre Burner | N.V. Acotech S.A | exploited by Acotech for Industrial Radiant Infrared Applications |
| Information on Limitations of Design Options for a Non-premixed Radiant Burner | Danish Gas Technology Centre | Non-exploitable Result (Technical reasons) |
| Use of Finned Surfaces for Flue Gas Heat Exchangers | Katholieke Universiteit Leuven | - Dissemination to third parties<br>- Consultancy |
| Technique for Rapid Assembly of Modular Ceramic Heat Exchanger for Use at High Temperature | BG plc | Examine options with potential HX**/recuperator suppliers, or possibly burner companies to commercialise |
| Reaction Bonded Silicon Carbide High Temperature Heat Exchanger Performance Data | BG plc, Gaz de France | Use data-sets to refine model and validate design tools for commercial heat exchanger |
| Self Bonding of Ceramic Components | BG plc | Non-exploitable result |
| Self Recuperative Gas-fired Confined Radiant Surface Burners | Gaz de France, Acotech, BG plc | Possible commercial exploitation |

**Table 6.1: Exploitation plans concerning the results of the project**

## 7. REFERENCES


[1] Tiekstra, G.C., "Report on the Design and Experimental Validation of Safety Devices that will Reduce the Explosion Risks for Premix Radiant Surface Burners", Clean and Efficient Energy Coversion Processes (CECON-project), Contract JOE3-CT95011

[2] Harris, R.J., "The investigation and control of Gas Explosions in buildings and heating plant", British Gas, E&F Spon Ltd, 1983

[3] Shirvill, L.C. 1986. "Metallic Fibre surface Combustion Radiant Gas Burners". Proceedings of the International Gas Research Conference, Toronto, pp. 837-844.

[4] Golombok, M. and Shirvill, L.C. 1988. "Laser flash Thermal Conductivity Studies of Porous Metal Fibre Materials". Journal of Applied Physics. Vol. 63. 63(6), pp. 1971-1976.

[5] Flamme M. 1992. "Test of a Cylindrical Perforated Metal Fibre Burner in a Condensing Boiler of 180 kW". Research Report. Gasw rme-Institut Essen, Germany. Doc 08/01, pp. 1-10.

[6] Vansteenkiste, P. 1995 Metal Fibre Burners, "Advanced Combustion Technology for Radiant Heat and Low NO Applications". Gasw rme International. July/August 1995, pp. 386-387.

[7] Andersen, P., Myken, A.N., Rasmussen, N.B., "Development of a non-premix radiant burner, Evaluation of design possibilties",Hørsholm: Danish Gas Technology Centre a/s, 1996, JOE3-CT95-0011

[8] Andersen, P., Myken, A.N., Rasmussen, N.B.,"Development of a non-premix radiant burner, Experimental results", Hørsholm: Danish Gas Technology Centre a/s, 1997, JOE3-CT95-0011

[9] Myken, A.N., Rasmussen, N.B., "Comparison/verification of advanced numerical tools for flow calculations", Hørsholm: Danish Gas Technology Centre, 1993. ISBN 8777950259 EFP-89 nr. 1323/8918

[10] Jørgensen, K., Myken, A.N., Rasmussen, N.B., "Test Furnace for Radiant Burners", Hørsholm: Danish Gas Technology Centre, 1996.

[11] Jørgensen, K., Rasmussen, N.B., Myken, A.N., "Selective Emittance Radiant Burners - An Experimental Investigation", Hørsholm: Danish Gas Technology Centre, 1996.

[12] W. Kays and A. London, "Compact Heat Exchangers", McGraw Hill, 1984.

[13] S. Kakac, R. Shah and W. Aung,,"Handbook of Single Phase Convective Heat Transfer", Wiley, 1987.

[14] E Van den Bulck, "Thermal design of flue gas heat exchangers", ASME HTD 314, pp. 49-56.

[15] S.J.Matthews, I.Alliat; "Task 5A - Materials Testing", Clean & Efficient Energy Conversion Processes (CECON Project), Contract JOE 3-CT95011.

[16] A.J.Jickells, S.Khela, I.Alliat and A.Segall; "Comparative study of test methodologies for thermal shock and thermal fatigue testing of ceramics in high temperature energy applications",Proceedings of the 2nd International Conference on Ceramics in Energy Applications, Institute of Energy, London, UK, 20-21 April, 1994, p253

[17] S.Khela, A.J.Jickells and S.J.Matthews; "The thermalcycling performance of ceramics for gas-fired furnaces", ibid, p273

[18] M.Maeda, K.Nakamura and A.Tsuge; "Scale effect of the testing furnaces on the oxidation of silicon carbide ceramics".J. Mater. Sci Lett., Vol.8, 1989, p144-46

[19] S.J.Matthews; "Task 5A - Report on Materials Selection for Compact High Temperature Heat Exchangers",Clean & Efficient Energy Conversion Processes (CECON Project), Contract JOE 3-CT95011.

[20] E. van den Bulck; "Task 4 - Modelling of the Ceramic Heat Exchanger",Clean & Efficient Energy Conversion Processes (CECON Project), Contract JOE 3-CT95011, Mid-Term report, February 1996 - January 1997.

[21] S.J.Matthews; "Task 5B - Joining & Fabrication Of Heat Exchanger", Clean & Efficient Energy Conversion Processes (CECON Project), Contract JOE 3-CT95011.

[22] K.D.Shepherd, J.Warren, S.Matthews; "Task 5D - Experimental Testing", Clean & Efficient Energy Conversion Processes (CECON Project), Contract JOE 3-CT95011.

[23] F.Kreith; "Principles of Heat Transfer-Second Edition", Internatinal Textbooks in Mechnical Enginering, p496-504

[24] K.D.Shepherd; "Task 5C - Heat Exchanger Design & Simulation".Clean & Efficient Energy Conversion Processes (CECON Project), Contract JOE 3-CT95011(Confidential Report).

[25] P. VANSTEENKISTE, "Final Report Task 2 : Development of the Premix Radiant Surface Burner", September 1997, Clean and Efficient Energy Conversion Processes (CECON-project), Contract JOE 3-CT95011 (Confidential Report).

[26] M-J. FOURNIGUET, "Task 6 : Validation of the bumers with internal recuperation", April 1998, Clean and Efficient Energy Conversion Processes (CECON- project), Contract JOE 3-CT95011.

[27] Colloque Recherche gazière Industrie, “L’infrarouge dans l’industrie : de l’innovation à l’offre de services”, GAZ DE FRANCE (CEGIBAT n°2.46.1.165)